The Casimir force: background, experiments, and applications



2005 Rep. Prog. Phys. 68 201

(http://iopscience.iop.org/0034-4885/68/1/R04)

INSTITUTE OF PHYSICS PUBLISHING REPORTS ON PROGRESS IN PHYSICS

Rep. Prog. Phys. **68** (2005) 201–236 doi:10.1088/0034-4885/68/1/R04

# The Casimir force: background, experiments, and applications

**Steven K Lamoreaux**

Los Alamos National Laboratory, University of California, Physics Division P-23, M.S. H803, Los Alamos, NM 87545, USA

Received 22 June 2004, in final form 14 September 2004
Published 30 November 2004
Online at stacks.iop.org/RoPP/68/201

**Abstract**

The Casimir force, which is the attraction of two uncharged material bodies due to modification of the zero-point energy associated with the electromagnetic modes in the space between them, has been measured with per cent-level accuracy in a number of recent experiments. A review of the theory of the Casimir force and its corrections for real materials and finite temperature are presented in this report. Applications of the theory to a number of practical problems are discussed.

  

**Contents**

## 1. Introduction

The force between uncharged conducting surfaces, the so-called 'Casimir force', was described by Schwinger as one of the least intuitive consequences of quantum electrodynamics. For conducting parallel flat plates separated by a distance $d$, this force per unit area has the magnitude [1]

$$\frac{F(d)}{A} = \frac{\pi^2}{240}\frac{\hbar c}{d^4} = 0.013\frac{1}{d^4}\mathrm{dyn}(\mu m)^4\, cm^{-2}. \tag{1}$$

This relationship can be derived by consideration of the electromagnetic mode structure between the two plates, as compared with free space, and by assigning a zero-point energy of $\frac{1}{2}\hbar\omega$ to each electromagnetic mode (photon). The change in total energy density between the plates due to modification of the mode structure compared with free space, as a function of the separation, $d$, leads to the force of attraction. This result is remarkable partly because it was one of the first predictions of a physical consequence directly due to zero-point fluctuations, and was contemporary with, but independent of, Bethe's treatment of the Lamb shift. Although the existence of this force was predicted over half a century ago, it has been measured to high accuracy (per cent level) only recently, within the last eight years.

The only fundamental constants that enter equation (1) are $\hbar$ and $c$; the electron charge, $e$, is absent, implying that the electromagnetic field is not coupling to matter in the usual sense. Perhaps this is stating the obvious, but the plates impose boundary conditions on the field and so their microscopic properties, in the limit of perfect conductivity, are not important. The role of $c$ in equation (1) is to convert the electromagnetic mode wavelength to a frequency, while $\hbar$ converts the frequency to an energy.

The term 'Casimir effect' is applied to a number of long-range interactions, such as those between atoms or molecules (retarded van der Waals interaction) and an atom and a material surface (Casimir–Polder interaction) and the attraction between bulk material bodies. The latter effect is generally referred to as *the* Casimir force and depends only on the bulk properties of the material bodies under consideration. This report will be limited primarily to a discussion of, and literature references to, *the* Casimir force because this forms a complete and distinct subject among the various Casimir effects. This report will also be limited primarily to applications in the realm of electromagnetism; as is well-known, the basic idea that the boundaries of a system can affect its physical properties has far-reaching consequences from condensed matter studies to quantum chromodynamics. (See [2–4] for reviews of the broader applications.) More specific reviews are presented in [5], in [6], which was compiled in honour of Dr Casimir's 80th birthday, and in [7], in honour of his 90th birthday. The most comprehensive recent review of the field is given in [8].

This report will give a background discussion on the meaning of the Casimir force, which remains controversial, i.e. does it prove that the electromagnetic field contains zero-point energy? An overview of theoretical and experimental developments over the last five years or so will be provided. Finally, applications of the Casimir force to some unusual and not-widely-appreciated physical situations will be discussed. The breadth of the field is so great that a comprehensive review of the literature is no longer possible or desirable in a single work [9].

The view that *the* Casimir force is simply the long-range (retarded) van der Waals interaction between material bodies is not accurate because the effect of the material boundaries must be considered in the calculation of the force. Furthermore, the van der Waals interactions between particles is non-additive, with the deviation increasing with density. Even in the case of three molecules, the van der Waals interaction is modified [10]. However, as shown in [5] (pp 249–51), a reasonable estimate of the Casimir force can be obtained by considering the pairwise interactions between the molecules contained in parallel plates with the polarizability

determined from the dielectric constant, $\epsilon$, and the Clausius–Mosetti relation. In the limit of $\epsilon \to \infty$, a $1/d^4$ force law with magnitude about 80% of Casimir's result is obtained. The lack of additivity is further addressed in [5], pp 254–8.

As mentioned above, one manifestation of a Casimir effect has its origin in molecular (van der Waals or dispersion force) interactions; this is the force of attraction between dielectric bodies which, in the case of tenuous media, can be interpreted as arising from the retarded $(1/r^7)$ and short-range $(1/r^6)$ van der Waals potentials between the molecules that make up the bodies, as was first discussed by London [11]. When the bodies are sufficiently dense, it is no longer valid to consider molecule–molecule interactions alone, and one must take into account the boundary conditions for the electromagnetic fields at the material surfaces and intermolecular effects. Lifshitz [12][1] first developed in 1956 the theory for the attractive force between two plane surfaces made of a material with a generalized susceptibility. His work was motivated by experimental results from force measurements between dielectric bodies that were much smaller than expected due to van der Waals interactions alone [13, 14]. Remarkably, the Lifshitz result does not explicitly involve a body's molecular properties; the attractive force is a function of only bulk material properties and the separation between the planes. The commentary in [14] indicates that before the Lifshitz analysis, it was expected that solid body force measurements would directly measure intermolecular forces, effectively amplified by the sheer number of participating pairs. The Lifshitz result indicates the importance of the boundaries, and in the limit of high density it is no longer possible to discuss the problem in terms of pair interactions.

For the case of perfect conductivity (near infinite electrical permittivity) the Lifshitz result is identical to equation (1), i.e. the force of attraction is independent of the electron charge or properties of the material bodies. The simplicity of the Casimir derivation leads one to ascribe a certain reality to electromagnetic field zero-point fluctuations, implying that the Casimir force is an intrinsic property of space. However, there is a point of view that the attractive force is due only to the interactions of the material bodies themselves, as implied by the Lifshitz derivation. There is a considerable body of literature concerning the source of the Casimir force (see [5] for an extensive discussion). This point is further discussed in section 2.3. Because the Casimir and Lifshitz approaches are in some respects at the opposite extremes, a brief discussion of the fundamentals of the Lifshitz calculation is relevant. However, the reader should be warned that the Lifshitz calculation is mathematically complicated; Ginzberg ([5], footnote p 233) comments that the calculations are 'so cumbersome that they were not even reproduced in the relevant Landau and Lifshitz volume ([15], chapter 9) where, as a rule, all important calculations are given'. (The calculations, using Green's function techniques, are presented in [16], chapter 13, while the original chapter 9 of [15] has been deleted from the most recent editions.) The complexity of the calculations are sufficiently great for the validity of the Lifshitz result to have been initially doubted, but the same result was eventually obtained using a number of more transparent methods (see [5], chapter 7, [17]).

For real materials, equation (1) must break down when the separation, $d$, is so small that the mode frequencies are higher than the plasma frequency (for a metal) or higher than the absorption resonances (for a dielectric) of the material used to make the plates; for sufficiently small separation, the force of attraction varies as $1/d^3$, as discussed in particular by Lifshitz [12]. In analogy with the attractive forces between atoms, the force in this range is sometimes referred to as the London–van der Waals attraction, while the $1/d^4$ range is referred to as the retarded van der Waals (Casimir) interaction. For the Casimir force, the crossover

[1] A typographical error in equation (1.13) should be noted (in the equation for $w_z$, the argument of the exponential has the wrong sign, both in the original article and in the translation).

distance between the regimes is $d \sim 100\,\text{nm}$, much larger than the atomic spacings in the materials, and so it still makes sense to describe the materials by their bulk properties (index of refraction); the $1/d^3$ versus $1/d^4$ interaction is in this case due to the truncation of the mode frequencies that are affected by the changing plate separation. Therefore the crossover between the two regimes appears to be of physically different origin compared with the case of the attractive forces between isolated atoms. Of course, when the plates are sufficiently flat and clean, when they are brought together the force does not go to infinity, but the plates fuse together with molecular or atomic bonding. When this bonding occurs, the maximum energy from the attractive force has been extracted.

The Casimir force and its calculation represent an electromagnetic waveguide problem, where imperfect materials are used in the construction of the waveguide. The zero-point fields are those associated with the waveguide; these modes do not exist in free space, and so the idea that the Casimir force represents a negative energy density compared with free space is controversial. It has also been suggested that the Casimir force might be a source of unlimited energy. Negative energy might be a necessary ingredient for time travel [18], and so the Casimir force has attracted some popular attention. As described in this report, the source of the Casimir force can be interpreted as due to fluctuations of charges within the material body; in the context of this picture, the negative energy idea can be questioned. In addition, Hawking further points out that zero-point fluctuations would lead to the rapid collapse and dissipation of a cosmic 'worm hole'. Finally, the Casimir force might be thought of as a 'precursor' to chemical bonding, that is the long-range attractive force that eventually leads to chemical combination. The amount of energy available from the long-range part of the chemical energy is infinitesimal compared with the full bonding energy (see [19]).

Given that the distances where the force of attraction is sufficiently strong to be experimentally detected are $d \sim 1000\,\text{nm}$ or less, the frequencies of interest are in the infrared and optical ranges. Thus an accurate theoretical description of an experimental system must take into account the optical properties of the plate material, as will be discussed later in this report.

There have been only a few dozen published experimental measurements of the Casimir force, to be compared with more than 1000 theoretical papers on the subject. Perhaps very few doubt the strict validity of equation (1) or its modification for real materials as derived in [12]. Because of the unavoidable uncertainties in bulk material and surface properties, verification of equation (1) as a test of QED will likely always be inferior to measurements of the Lamb shift or $g - 2$ of the electron. However, Casimir's idea remains central to theoretical physics, as evidenced by the exponential growth of references to his original paper, as illustrated in figure 1 (after [5]).

Only recently have measurements of the Casimir force with accuracy at the per cent-level of precision become possible. However, the existence of short-range cohesive forces has been recognized since the earliest days of modern physics. Cavendish [20] considered this a possible correction to his measurements of the gravitational constant, as discussed in his 1798 publication describing his work which marks the beginnings of modern experimental science:

> Another objection, perhaps, may be made to these experiments, namely, that it is uncertain whether, in these small distances, the force of gravity follows exactly the same law as in greater distances. There is no reason, however, to think that any irregularity of this kind takes place, until the bodies come within the action of what is called the attraction of cohesion, and which seems to extend only to very minute distances.

Cavendish tested whether there was an anomalous force at small separations, and found none. So not only did Cavendish set a possible limit on the magnitude of the Casimir force, but also

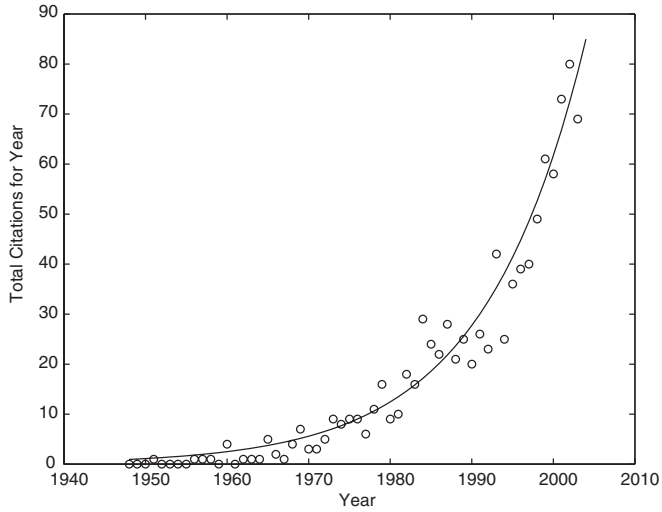


**Figure 1.** Number of citations per year of Casimir's 1948 paper. The time constant of exponential increase is about 12 years.

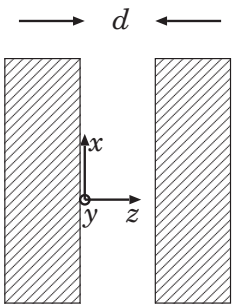


**Figure 2.** Coordinate system for calculating the Casimir force.

on other possible forces that are again the *nouvelle vague* in the context of string and particle field theories.

## 2. Source of the Casimir force

### *2.1. Casimir's calculation [1]*

The geometry for calculation of the Casimir force is shown in figure 2. For perfectly conducting plates, the boundary condition is that the parallel component of the electric field is zero at the surfaces of the plates. This places a quantization on $k_z$:

$$k_z = \frac{n\pi}{d}, \tag{2}$$

while $k_x$ and $k_y$ are continuous in the case of plates of large area. The zero-point energy is calculated by assigning $\hbar\omega/2$ to each mode,

$$E(d) = 2 \sum_{k_x,k_y,k_z}{}' \frac{\hbar\omega_{kx,ky,kz}}{2} = \sum_{k_x,k_y,n}{}' \pi\hbar c\sqrt{k_x^2 + k_y^2 + \frac{n^2\pi^2}{d^2}}, \tag{3}$$

where the factor of 2 is for the two polarization modes, and the prime on the sum indicates that there is only one polarization state for the $n = 0$ mode where the electric field is perpendicular to the plates. The sum over $k_x$ and $k_y$ is replaced by an integral, $\sum_{k_x} \to (L/\pi)\int_0^\infty \mathrm{d}k_x$, and similarly for $k_y$. If $d$ is made arbitrarily large, the sum over $n$ can also be replaced by an integral.

The Casimir force is determined by the change in energy when the plates are at finite $d$ and when $d \to \infty$, which determines the potential energy

$$U(d) = E(d) - E(\infty) = \hbar c \frac{L^2}{\pi^2}\int_0^\infty\int_0^\infty \mathrm{d}k_x\,\mathrm{d}k_y\Bigg[{\sum_n}'\sqrt{k_x^2+k_y^2+\frac{n^2\pi^2}{d^2}} - \frac{d}{\pi}\int_0^\infty \mathrm{d}k_z\sqrt{k_x^2+k_y^2+k_z^2}\Bigg]. \tag{4}$$

Now Casimir's trick was to introduce a cutoff function, $f(\omega/c) = f(k) = f((k_x^2 + k_y^2 + k_z^2)^{1/2}$, which has the property that $f(k) = 1$ for $k \ll k_m$ and $f(k) = 0$ for $k \gg k_m$, where $ck_m \approx \omega_\mathrm{p}$, the plasma frequency for the metal costituting the plates. Using polar coordinates to specify $k_{x,y}$ with $k = \sqrt{k_x^2 + k_y^2}$ and substituting $x = k^2d^2/\pi^2$ and $\kappa = k_z d/\pi$,

$$U(d) = \left[\frac{\pi^2\hbar c}{4d^3}\right]L^2\left[\frac{1}{2}F(0) + \sum_{n=1}^\infty F(n) - \int_0^\infty \mathrm{d}\kappa\,F(\kappa)\right], \tag{5}$$

where

$$F(\kappa) = \int_0^\infty \mathrm{d}x(x+\kappa^2)^{1/2} f\left(\left(\frac{\pi}{d}\right)(x+\kappa^2)^{1/2}\right). \tag{6}$$

The potential energy can be calculated by use of the Euler–Maclaurin summation formula [21],

$$\sum_{n=1}^\infty F(n) - \int_0^\infty \mathrm{d}\kappa\,F(\kappa) = -\frac{1}{2}F(0) - \frac{1}{12}F'(0) + \frac{1}{720}F'''(0) + \cdots, \tag{7}$$

if $F(\infty) = 0$. The derivatives can be calculated by noting that

$$F(\kappa) = \int_{\kappa^2}^\infty \mathrm{d}u\sqrt{u}\,f\left(\left(\frac{\pi}{d}\right)\sqrt{u}\right) \to F'(\kappa) = -2\kappa^2 f\left(\left(\frac{\pi}{d}\right)\kappa\right) \tag{8}$$

by the fundamental theorem of calculus. Assuming that all derivatives of the cutoff function go to zero as $\kappa \to 0$, the only contribution is the $F'''(0)$ term; therefore

$$U(d) = \left[\frac{\pi^2\hbar c}{4d^3}\right]L^2 \times \frac{-4}{720} = -\left[\frac{\pi^2\hbar c}{720d^3}\right]L^2 \tag{9}$$

and calculating the force as $-\mathrm{d}U(d)/\mathrm{d}d$ reproduces equation (1).

The interesting point of this calculation is that the specific form of the cutoff function does not enter. Introducing the cutoff function makes the otherwise divergent integral vanish, and so it is tempting to believe that the cancellation would occur without the cutoff. An alternative point of view is that there are no zero-point excitations of the fields near the plates for frequencies much higher than $\omega_\mathrm{p}$. It can be shown that the dominant contribution to the force occurs at $k \approx 1/4d$, with contributions from higher $k$ falling off exponentially. So for large separations it is not surprising that the result does not depend on $\omega_\mathrm{p}$.

### 2.2. Lifshitz calculation

The Lifshitz calculation [12] is developed from Rytov's theory [22] of charge and current fluctuations in a material body. These fluctuations serve as a source term for Maxwell's equations, i.e. classical fields, subject to the boundary conditions presented by the body surfaces. These fluctuations, as described in [22], are a result of Johnson noise in a dissipative medium, and can be understood from the following considerations. If a small cubical volume cell $\Delta V = L^3$ inside one of the bodies is taken, the current and electric polarization fluctuations within that volume can be determined by use of the fluctuation–dissipation theorem [23, 24].

Any specific material body has a frequency-dependent complex electromagnetic permittivity (which is called the dielectric constant in the case of non-conducting bodies) $\epsilon(\omega) = \epsilon'(\omega) + i\epsilon''(\omega)$, where the imaginary part of $\epsilon$ leads to dissipation of the electromagnetic energy in the material body. (It is assumed here that the magnetic permeability is unity.) In the case of a conductor with static electrical conductivity $\sigma$, $\epsilon(\omega) = 4\pi i\sigma/\omega$ (using Gaussian units for this and subsequent equations). Consider a current $I$ from one cube face to the opposite one; as the current flows, charge will accumulate on either face, leading to an electrical polarization across the cube, 90° out of phase with the current. The electrical resistance across the cell is $R = 1/\sigma L$; from the fluctuation–dissipation theorem, the random current spectral density is

$$|I(\omega)|^2 = \frac{\hbar\omega}{\pi} R^{-1} \left[ \frac{1}{2} + \frac{1}{e^{\hbar\omega/kT} - 1} \right], \tag{10}$$

where $k$ is Boltzmann's constant and $T$ is the absolute temperature. (This can be derived by analogy with a harmonic oscillator, with charge $Q$ and current $I$ analogous to the conjugate variable's position $x$ and momentum $p$.)

The oscillating current, $I(\omega)$, will lead to an oscillating charge, $Q(\omega)$, per unit area (total area $L^2$) on either side of a cell, and this represents an electric polarization field $K(\omega) = Q(\omega)/L^2$ within the cell. Because $I(\omega) = \dot{Q}(\omega)/4\pi$, the magnitude of the charge fluctuation is $|Q| = 4\pi|I|/\omega$. (In the case of a non-conducting dielectric with absorption, this argument also applies because the absorption will lead to a fluctuating polarization that can be interpreted as a current.) The spectral density of the electrical polarization within a small cell is therefore

$$\begin{aligned} |K(\omega)|^2 &= \frac{|4\pi Q(\omega)|^2}{(\omega L^2)^2} \\ &= 4\hbar \left[ \frac{4\pi\sigma}{\omega} \right] \frac{1}{L^3} \left[ \frac{1}{2} + \frac{1}{e^{\hbar\omega/kT} - 1} \right] \\ &= 2\hbar\epsilon'' \coth \frac{\hbar\omega}{2kT} \frac{1}{L^3}. \end{aligned} \tag{11}$$

It can be assumed that the electrical fluctuations (that is, electrical charge movement due to thermal fluctuations as opposed to that driven by a field generated external to the cell) between the three sets of opposite cube faces are uncorrelated, and that fluctuations at different cells in the bodies are uncorrelated. These assumptions are valid for a material with a linear electrical response, implying that the magnitude and spectrum of the fluctuations are unaltered by fields in the body. Furthermore, as $\Delta V \to 0$, $1/L^3 = \delta(\vec{r} - \vec{r}')$, where $\vec{r}'$ labels the cell location. Labelling the directions across the cube as $i$, $j$, $k$, the average polarization fluctuation spectral density can be written as

$$\overline{K_i^\omega(\vec{r}) K_j^\omega(\vec{r}')} = 2\hbar\epsilon'' \coth \left[ \frac{\hbar\omega}{2kT} \right] \delta_{ij} \delta(\vec{r} - \vec{r}'). \tag{12}$$

This is the Lifshitz calculation source term. The fluctuations persist at $T = 0$, and appear to be associated with the material body, in contrast to Casimir's calculation, where the fluctuations were associated with the electromagnetic field.

In this analysis, a linear electrical response was taken, implying that the fluctuating fields do not modify the material properties. The modifications of non-additivity in the pairwise interactions of the molecules of a body are accounted for in the bulk electrical properties of the material. Unfortunately, these properties are difficult to calculate from first principles or molecular properties, and so properties of relevance to accurate determination of the Casimir force must, to a large degree, be measured by experiment.

In light of more transparent calculational techniques, further commentary on the Lifshitz paper is not warranted, but it remains one of the most elegant works in the history of mathematical physics.

### *2.3. Identification of the source of the Casimir force*

The calculation of the Casimir force in terms of changes in the zero-point energy of the electromagnetic field energy seems so natural that the Casimir effect has been generally taken as proof of the reality of the zero-point electromagnetic vacuum field energy. However, Schwinger *et al* [25] produced a derivation of the Casimir force from a theory for which there are no nontrivial vacuum fields, and Milonni [26] has produced a derivation without reference to the vacuum radiation field. The fact that the Casimir force can be largely explained by the van der Waals pairwise interaction between molecules in the plates, which can be calculated without reference to the electromagnetic vacuum field, along with Schwinger and Milonni's considerations, indicates that the Casimir force is not sufficient proof for the existence of the zero-point of the electromagnetic vacuum field.

The approaches in Casimir and Lifshitz calculations directly illustrate the problem in ascribing the source of the Casimir force to the zero-point vacuum field. The Lifshitz calculation makes use of the fluctuation–dissipation theorem which is based on the energy storage in an electric field, and in a certain sense, the quantization of the stored energy indirectly implies that the zero-point of the electromagnetic field modes is automatically filled to a minimum energy of $\hbar\omega/2$ for every mode; however, the Lifshitz calculation of the attractive force does not require quantization of the electromagnetic field, and in this respect is analogous to the Planck analysis of the black body spectrum; one cannot decide whether the quantization lies in the fluctuation spectrum of the material body, or with the electromagnetic field [27]. On the other hand, Casimir assigned a certain reality to the zero-point excitations by his assumption of $\hbar\omega/2$ energy for each mode in his calculation. The two approaches represent different realizations of the same phenomenon; they have in fact been shown to be identical ([28–30]. As stated by Milonni, interpretation of the Casimir force in terms of the vacuum field is a matter of taste ([5], pp 250–1).

However, the question of whether zero-point fluctuations of the free-space electromagnetic field exist might be moot. Milne suggests that space is not an object, but a map invented to describe the location of objects: 'It is an unreflecting person who views space as a visible emptiness' [31]. The point is that our universe contains matter; a region of unconnected emptiness is elsewhere—the very presence of matter within our observable universe implies an excitation of the electromagnetic field, if there is to be equilibrium between the matter and the electromagnetic field at zero temperature, in which case the field excitation is the zero-point energy. As an aside, Milne's model of the universe is accepted as valid for an empty universe [32]; is a universe that contains zero-point fluctuations empty, or do zero-point fluctuations lead to a gravitational potential? These questions have vexed modern physics,

and led Pauli to reject the notion of zero-point energy, at least in the case of the free-space quantized electromagnetic field [33, 34]; the energy density due to the zero-point excitations of the eletromagnetic field exceeds $10^{60}\,\mathrm{g\,cm^{-3}}$, depending on the cutoff, as discussed in [35]. This zero-point energy density has to be incorporated into general relativity, where it acts in effect as a cosmological constant as introduced by Einstein to produce a static solutions of his field equations. Astronomical data indicate that the cosmological constant is many orders of magnitude smaller than implied by the enormous pressure due to zero-point excitations [36], and this difficulty remains unresolved.

The source of the Casimir force, and zero-point field excitations, is eloquently stated by Lifshitz [12]:

> We can however approach this problem in purely macroscopic fashion . . . From this point of view, the interaction of the objects is regarded as occurring through the medium of the fluctuating electromagnetic field which is always present in the interior of any absorbing medium, and also extends beyond its boundaries—partially in the form of travelling waves radiated by the body, partially in the form of standing waves which are damped exponentially as we move away from the surface of the body. It must be emphasized that this field does not vanish even at absolute zero, at which point it is associated with the zero-point vibrations of the radiation field.

Perhaps it should be added that the fluctuating field could be associated with the zero-point motion of electrons within the body. Under the circumstances, the term 'molecular' in the title of [12] might have been better left out. We can guess that this work, the title in particular, was directed towards experimental measurements between material bodies which were expected to determine the molecular van der Waals potential, as described above. As Lifshitz states, 'In the limiting case of rarefied media, the method must of course lead to the results as are obtained by considering the interactions of individual atoms', the point being that the attractive (Casimir) force between extended dense bodies tells us little with regard to the (retarded) van der Waals interaction between individual atoms and provides no direct proof of the existence of a zero-point vacuum field.

The Casimir force can be thought of as an emergent collective phenomenon; all calculations in fact leave out details of field quantization and its interaction with matter, and calculate the electromagnetic field from its bulk response to matter which always includes some dissipation. This dissipation ensures that the fields are coupled to a thermal bath, which, even at absolute zero, still has energy associated with the zero point.

In concluding this introductory section, we see that the source of the zero-point excitation of the electromagnetic field is irrelevant in Casimir's calculation. There are physical phenomena that truly require a quantization of the electromagnetic field for their explanation; the Casimir force is not among these phenomena, because the predictions based on the different points of view are identical.

## 3. Calculational techniques

### *3.1. Van Kampen et al's technique*

The idea that a sum can be converted into a complex contour integral is described in [37] (p 413), and has broad applications in all branches of physics. In the case of the Casimir force, the techniques were first used in [38]. A brief outline of the technique is presented here (see [5], chapter 7 for details). (Green's function techniques, described in [16], section 81, will not be reviewed here.)

The electromagnetic wave propagation vectors in, and perpendicular to, the surfaces (vacuum, plates) shown in figure 2 are

$$K_i^2 = k^2 - \epsilon_i(\omega)\frac{\omega^2}{c^2}, \tag{13}$$

where $k$ is a real number, and $i = 0, 1$, with 0 ($\epsilon_0(\omega) = 1$) representing the space between the plates and 1 representing the plates, with the requirement $\mathrm{Re}(K_i) \geqslant 0$. The possibility of a complex $\epsilon_1$ must be allowed for, in which case $K_i$ can be complex. In section 3.3, the use of the technique in the case of absorption (complex $\epsilon$) is justified. The real number $k$ is the Fourier variable for describing fluctuations that vary as a function of position in the direction parallel to the plate surfaces. It should be noted that $k$ and $\omega$ are independent variables, and only when $\omega/k \leqslant c$ can we think of the waves as propagating; otherwise they are evanescent or 'above the light cone'.

There are two type of solutions to the wave equation, one with the electric vector parallel (*TE* or *H* waveguide modes) to the surfaces (with arbitrary orientation chosen as the $y$ axis, in which case the $x$ dependence of the fields is $\mathrm{e}^{\mathrm{i}kx}$), $e_y(z)$, and one with the electric vector perpendicular (*TM* or *E* waveguide modes) to the surfaces (taken as the $z$ axis), $e_z(z)$. The wave equation in the $z$ direction is

$$\frac{\mathrm{d}}{\mathrm{d}z}e_{y,z}(z) - K_i^2 e_{y,z}(z) = 0 \tag{14}$$

and the boundary condition for $e_z$ is that $\mathrm{d}e_z/\mathrm{d}z$ and $\epsilon e_z$ be continuous, while for $e_y$ it is that $\mathrm{d}e_y/\mathrm{d}z$ and $e_y$ be continuous. Ignoring unphysical exponentially growing solutions, the solutions are

$$\begin{aligned} e_{y,z}(z) &= A\mathrm{e}^{K_1 z} && z < 0 \\ &= B\mathrm{e}^{K_0 z} + C\mathrm{e}^{-K_0 z} && 0 \leqslant z \leqslant d \\ &= D\mathrm{e}^{-K_1 z} && z > d, \end{aligned} \tag{15}$$

which lead to two sets of linear equations relating $A$, $B$, $C$ and $D$ for each of the two cases. The condition for nontrivial solutions of these equations is that the determinant of the coefficient matrix be zero, yielding the following two expressions. For TM modes,

$$\frac{(K_1 + \epsilon_1 K_0)^2}{(K_1 - \epsilon_1 K_0)^2}\mathrm{e}^{2K_0 d} - 1 = 0 = f_z(k, \omega, d), \tag{16}$$

while for TE modes,

$$\frac{(K_0 + K_1)^2}{(K_0 - K_1)^2}\mathrm{e}^{2K_0 d} - 1 = 0 = f_y(k, \omega, d). \tag{17}$$

The zeros, $\omega_{ny,nz}(k, d)$, of $f_{y,z}$ determine the allowed mode eigenfrequencies.

The zero-point energy associated with the plates is determined by assigning an energy $\hbar\omega/2$ to each mode,

$$E(d) = \sum_{n,\vec{k}}\left[\frac{\hbar\omega_{ny}(k, d)}{2} + \frac{\hbar\omega_{nz}(k, d)}{2}\right] \tag{18}$$

(in general, the eigenfrequencies are complex, but the imaginary parts cancel as discussed in section 3.2). The sum over $k$, in the continuum limit, becomes an integral,

$$\sum_{\vec{k}} \to \left(\frac{L}{2\pi}\right)^2 \int 2\pi k \, \mathrm{d}k, \tag{19}$$

where $L$ is the transverse dimension of the plate in the $x$, $y$ directions. As described in [37], the theory of complex functions can be employed to evaluate the sum over eigenfrequencies; specifically, according to the argument theorem [39, 40],

$$\frac{1}{2\pi i}\oint_C \frac{f'(z)}{f(z)}\mathrm{d}z = N - P, \tag{20}$$

where $C$ is a closed path in the complex plane, $N$ and $P$ are the numbers of zeros and poles within $C$, respectively, and the path is counterclockwise. The argument theorem can be modified to give the sum of the zeros and poles:

$$\frac{1}{2\pi i}\oint_C z\frac{f'(z)}{f(z)}\,\mathrm{d}z = \Big[\sum z_i\Big]_{f(z_i)=0} - \Big[\sum z_i\Big]_{f(z_i)=\infty}. \tag{21}$$

Furthermore, $f'(z)/f(z) = \mathrm{d}(\log f(z))/\mathrm{d}z$. The eigenfrequencies of physical interest lie in the right half plane; integrating along the imaginary axis from $\infty$ to $-\infty$ and closing the path with a semi-circle at infinity around the right half plane (see [5] for details) and integrating by parts gives

$$E(d) = \frac{\hbar L^2}{8\pi^2}\int_0^\infty k\,\mathrm{d}k\int_{-\infty}^\infty \mathrm{d}\xi[\log g_y(\xi,k,d) + \log g_z(\xi,k,d)] \tag{22}$$

with $\omega = \mathrm{i}\xi$, and $\xi$ is real, $g_{y,z}(\xi,k,d) = f_{x,y}(\mathrm{i}\xi,k,d)$, and

$$K_i = k^2 + \frac{\epsilon_i(\mathrm{i}\xi)\xi^2}{c^2}. \tag{23}$$

Finally, the poles of equations (16) and (17) do not depend on $d$ because it only enters in the multiplicative exponential; therefore, equation (22) gives the zero-point energy up to an additive constant, while the force per unit area is given by

$$F(d) = -\frac{\partial}{\partial d}E(d) = -\frac{\hbar}{4\pi^2}\int_0^\infty k\,\mathrm{d}k\int_0^\infty \mathrm{d}\xi\,K_0\left[\frac{1}{g_y(\xi,k,d)} + \frac{1}{g_z(\xi,k,d)}\right], \tag{24}$$

where (possibly) non-physical $d$-independent terms are omitted.

The Lifshitz result is obtained if the substitutions of new variables $p$ and $s$ are made, with $\epsilon_0 = 1$:

$$k^2 = \frac{\xi^2}{c^2}(p^2 - 1) \tag{25}$$

in which case $K_0^2 = k^2 + \xi^2/c^2$ or

$$K_0 = \frac{\xi}{c}p, \tag{26}$$

$$K_1 = k^2 + \epsilon_1\frac{\xi^2}{c^2} = \frac{\xi^2}{c^2}[p^2 - 1 + \epsilon_1] \equiv \frac{\xi^2}{c^2}s_1^2 \tag{27}$$

and equation (24) becomes

$$F(d) = -\frac{\hbar^2}{2\pi c^3}\int_1^\infty \mathrm{d}p\,p^2\int_0^\infty \mathrm{d}\xi\,\xi^3\left[\frac{1}{g_y(s,p,d)} + \frac{1}{g_z(s,p,d)}\right]. \tag{28}$$

In the case of perfect conductors,

$$g_x(s,p,d) = g_y(s,p,d) = \mathrm{e}^{2\xi pd} - 1 \tag{29}$$

and the integrals can be easily done by use of the substitution $y = 2\xi pd/c$,

$$F(d) = -\frac{\hbar}{2\pi^2c^3d^4}\int_1^\infty \mathrm{d}p\,p^{-2}\int_0^\infty \frac{\mathrm{d}y\,y^3}{\mathrm{e}^y - 1} = -\frac{\pi^2\hbar c}{240d^4}, \tag{30}$$

which is Casimir's result.

### *3.2. Extensions of the technique*

As discussed by Milonni [5], the contour integration technique used to sum the eigenfrequencies appears to be technically correct only if the eigenfrequencies lie on the positive real axis. There has been much commentary on the extension of this technique to absorptive materials (i.e. complex permittivity), in which case the eigenfrequencies are complex. Barash and Ginzburg [41] introduced the idea of an auxiliary system to account for the complex permittivity, with the fundamental eigenfrequencies real. Further commentary is provided by Tomas [42] and Raabe *et al* [43], who assert that electromagnetic modes in the presence of absorption cannot be defined, and calculate the force without reference to the fundamental system modes. Lifshitz's calculational technique and Green's function techniques ([16], section 81) circumvent the problem of defining modes in the presence of absorption, and these techniques are generalized in [42,43].

However, the contour integration method gives the correct answer quite simply, and agrees with all other calculational techniques; e.g. the mathematics does not know about the auxiliary system as introduced by Barash and Gizburg. A non-rigorous explanation for why the technique works in the case of absorption can be developed from elementary considerations as follows.

First, the Van Kampen technique adds up the eigenvalues of a linear set of differential equations that are subjected to homogeneous boundary conditions; it is well-known that the eigensolutions are orthogonal (the Sturm–Liouville problem, [37], pp 719–29) and form a complete set of functions. Therefore the electromagnetic field within, and in the gap between the plates, can be described completely by these solutions, in the case of isotropic materials that have a linear and causal electromagnetic response. It is known experimentally (particularly in electronics and laser physics) that so long as the system is linear, there is no cross-coupling between non-degenerate modes, other than incoherently through the thermal bath. Dissipation to the thermal bath is a non-linear process (Joule heating), and the probability of transferring energy from a specific driven mode to another specific mode is vanishingly small by this process. All of this is to say that if a specific frequency field is supplied to a linear electromagnetic resonator, the steady-state response has no frequencies other than the drive frequency. This is not the case for a non-linear system. Experimentally, even in the case of dissipation, modes are well-defined for a linear system.

Next, for a generalized permittivity [15], $\epsilon(-\omega^*) = \epsilon^*(\omega)$. Therefore, the eigenfrequencies for the general boundary problem case occur in pairs, $\omega = \pm\omega' + \mathrm{i}\omega''$. Taking the case where $\mathrm{Re}(K_i)$ are either all positive or all negative which follows from continuation, as $\omega \to \infty$, all the $K_i$ become equal because $\epsilon_i(\omega) \to 1$. In the case where $\mathrm{Re}(K_i) > 0$, representing an exponentially damped surface wave, the eigenfrequencies lie in the lower half plane; therefore, $\mathrm{e}^{-\mathrm{i}\omega t}$ is damped exponentially in time. For $\mathrm{Re}(K_i) < 0$, the eigenfrequencies lie in the upper half plane and represent solutions growing exponentially in time and space. Clearly, the contour integration method as described above should not work without justification regarding branch cuts, etc.

The way around this problem is that instead of considering the eigenfrequencies, one can consider the corresponding eigenwavenumbers, $K_i$, and $K_0$ in particular. The eigenwavenumbers occur in complex conjugate pairs, $K_0 = K_0' \pm \mathrm{i}K_0''$ (as can be seen from equation (13) and the properties of $\epsilon(\omega)$ in the complex plane), and by definition the $K_i$ are in the right half plane for the exponentially damped solutions. Furthermore, writing the determinant function in terms of $K_0$, and using the fact that $K_0\,\mathrm{d}K_0 = -\omega\,\mathrm{d}\,\omega/c^2$, leads to

$$-c^2 \oint_C K_0 \frac{f'(\omega(K_0))}{f(\omega(K_0)}\,\mathrm{d}K_0 = \oint_C \omega(K_0)\frac{f'(\omega(K_0))}{f(\omega(K_0))}\,\mathrm{d}K_0 \tag{31}$$

and $\mathrm{d}K_0$ can be replaced by $\mathrm{d}\omega$ because the path is arbitrary in the complex plane (note that in the case of no absorption, the eigenvalues for $K_0$ lie on the imaginary axis, while those for

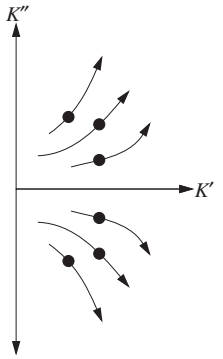


**Figure 3.** Motion of poles as a function of $d$.

$\omega$ lie on the real axis, and the contour must be adjusted accordingly). Because the eigenvalues for $K_0$ occur in conjugate pairs, the left-hand side of equation (31) is real; therefore, the sum in equation (18) is real, as can be seen from equation (21) when the integral is taken along the imaginary $\omega$ axis. As the plate separation, $d$, is made smaller, the poles move as shown in figure 3.

This analysis can also be applied to calculation of the Casimir force when the surface impedance is used to characterize the material bodies. The surface impedance has essentially the same character in the complex plane as the permittivity, and represents a generalized susceptibility.

In the case of a non-local susceptibility due to surface plasmons or non-local electron correlations (which occur when the electron mean free path exceeds the electromagnetic field penetration length in a conductor), specialized techniques are required for determining the noise current operator [44]. Calculations of the Casimir force in these situations have only recently received serious attention [45].

### *3.3. Applications to other geometries*

Casimir attempted to derive the fine-structure constant by constructing an electron model based on the assumption that an electron is a sphere of uniform charge density, with total charge equal to $e$, the electron charge. The radius of the sphere can be determined by a balance between the Casimir force (assumed attractive) that would tend to hold the electron together and the Coulomb repulsion that would tend to make the electron expand [46]. Further analysis by Boyer invalidates this model.

Motivated by Casimir's model, Boyer was the first to consider the Casimir force for a sphere and found a remarkable result: the vacuum stress outside the sphere tends to pull the sphere apart [47]. Apparently, there are greater number of modes on the sphere surface than in free space, and as the sphere diameter increases, the rate at which new modes appear on the surface is greater than the rate at which free-space modes disappear. In free space the modes are limited to those with a real propagation vector, while on the sphere surface, evanescent waves can exist [48]; these are exponentially damped waves, and the implication of the Boyer result is that these modes outnumber the free-space modes. There appears to be no *a priori* way of predicting the stress on a specific geometrical object. The most complete overview of this problem is given in [3].

It is unclear whether the two hemispheres that result if a sphere is cut in half would repel each other. Boyer's calculation was for the field stress outside a sphere. A sphere that is cut in half represents a different problem.

So far, all experiments done to address geometrical effects have been for theoretically trivial configurations. The effects can be fully understood from geometrical averaging, and a full electromagnetic mode calculation has not yet been required for interpreting the experimental results.

As an aside, the force between a dielectric and a magnetically permeable plate is repulsive [49]; a physical picture of this effect is given in [50]. The van der Waals-like interaction between magnetically permeable particles is also repulsive and Kleppner [51] gives a simple explanation of this effect.

The repulsive character in the case of magnetic permeability and the possibility of a repulsive Casimir force has been discussed recently because of its potential utility in nanoengineered systems [52]. Unfortunately, there are no materials with significant magnetic response at optical frequencies [53, 54].

## 4. Corrections

In its essential form, the Casimir force appears as beautifully simple, whereas in reality, conductors are imperfect. In fact, in his original article, Casimir truncated the divergent integral, having recognized that any realistic mirrors would not be effective for wavelengths in the ultraviolet or shorter range. Assuming a simple form for the conductivity, e.g. a free-electron plasma model, corrections for the finite conductivity can be obtained in a relatively simple form [55, 56]. However one must bear in mind that such models are only approximate.

Another source of correction is the surface roughness. In principle, one should solve the wave equation with rough boundaries to determine the effect of roughness, but in some situations a geometrical averaging can be used to approximate the correction; this has been the subject of a number of papers (section 4.5). One should be aware that the geometrical averaging has been done only for the Casimir force ($1/r^4$), while the finite conductivity correction has been expanded in additional multiplicative terms in $1/r^n$, and each of these terms has an average over the surface roughness different from that for the Casimir force; the simplistic theoretical analysis that has been done so far is inadequate for interpreting experimental results to high precision, although this has been attempted [57]. Under the circumstances, testing the theory of the Casimir force to much better than 10% seems a daunting task.

### *4.1. Imperfect conductivity*

Equation (1) must break down when the plate separation is so small that the mode frequencies being affected when $d$ is varied are above the material resonance or plasma frequencies. In the case of a simple metal, the real part of the dielectric constant can be approximated by

$$\epsilon'(\omega) = 1 - \frac{\omega_{\mathrm{p}}^2}{\omega^2}, \tag{32}$$

where $\omega_{\mathrm{p}}$ is the plasma frequency and is proportional to the effective free-electron density in the metal. It is convenient to introduce the plasma wavelength, $\lambda_{\mathrm{p}} = 2\pi c/\omega_{\mathrm{p}}$. Corrections to equation (1), expanded in terms of $\lambda_{\mathrm{p}}/d$, have been calculated to first order by Hargraves [58] and by Schwinger *et al* [55] and to second order by Bezerra *et al* [59] For flat plates, the corrected force can be written in terms of equation (1) with a multiplicative factor,

$$F'(d) = F(d)\left[1 - \frac{8}{3\pi}\frac{\lambda_{\mathrm{p}}}{d} + \frac{120}{4\pi^2}\left(\frac{\lambda_{\mathrm{p}}}{d}\right)^2\right]. \tag{33}$$

This equation is only valid for $\lambda_p/d \ll 1$; unfortunately, the Casimir force is large enough to be measured accurately experimentally only in the range $\lambda_p/d \approx 1$ or larger. We are also faced with the problem that equation (32) is only approximate.

It is, however, possible to determine very accurately the attractive force as a function of the plate separation by numerical calculation if its complex permittivity as a function of frequency is known:

$$\epsilon(\omega) = \epsilon'(\omega) + \mathrm{i}\epsilon''(\omega), \tag{34}$$

where $\epsilon'$ and $\epsilon''$ are real. With this information, the permittivity along the imaginary axis can then be determined using the Kramers–Kronig relation,

$$\epsilon(\mathrm{i}\xi) = \frac{2}{\pi}\int_0^\infty \frac{x\epsilon''(x)}{x^2+\xi^2}\,\mathrm{d}x + 1. \tag{35}$$

This can be used in the Lifshitz expression for the attractive force [12],

$$F'(d) = \frac{\hbar}{2\pi^2 c^3}\int_0^\infty\int_1^\infty p^2\xi^3\left(\left[\frac{[s+p]^2}{[s-p]^2}\mathrm{e}^{2p\xi d/c} - 1\right]^{-1} + \left[\frac{[s+\epsilon(\mathrm{i}\xi)p]^2}{[s-\epsilon(\mathrm{i}\xi p)]^2}\mathrm{e}^{2p\xi d/c} - 1\right]^{-1}\right)\mathrm{d}p\,\mathrm{d}\xi, \tag{36}$$

where $s = \sqrt{\epsilon(\mathrm{i}x/p) - 1 + p^2}$. The numerical calculations for the attractive force between Au, Al and Cu plates have been published [60], and significant deviations from equation (33) were found. In particular, for Al with $d \approx 100$ nm, equations (33) and (36) differ by about 5%; one should note that including the third order correction to equation (33) worsens the deviation. However, these calculations should be considered in light of the notorious variation of bulk and surface properties of materials due to preparation technique, purity, etc [61, 62]. Numerical errors in [60] are corrected in [63] and [64].

### *4.2. Surface roughness*

From the earliest experiments, it was realized that surface roughness would lead to an increase in the apparent Casimir force and therefore cause systematic errors in measurements aimed at verifying equation (1). Such effects were observed by van Blokland and Overbeek [61]; roughness has been discussed theoretically by van Bree *et al* [65] and more recently in [66].

For high-quality optically polished surfaces, the rms amplitude of the roughness $A$, is usually of the order of 30 nm or less. For a $1/d^4$ attractive force, the correction to equation (1) can be written as

$$F'(d) \approx F(d)\left[1 + 4\left(\frac{A}{d}\right)^2\right]. \tag{37}$$

The correction for a torsion balance experiment, at the point of closest approach, is about 1%, while for an atomic force microscopy (AFM) experiment, it is about 30%. These experiments are discussed in section 6.

The roughness correction was derived in the context of a $1/d^4$ force law (this can be easily modified for the spherical plate $1/d^3$ case). However, the finite conductivity correction, particularly as given by equation (33), effectively has terms containing $1/d^5$ and $1/d^6$. In principle, the roughness correction should be done for each power law separately, or the average force determined from the accurate calculation, equation (36). One should also bear in mind that the simple geometrical averaging procedure is not exactly correct; a complete treatment would involve solving the appropriate electromagnetic rough boundary problem. Furthermore, the geometrical averaging is correct so long as the period of the roughness is either much larger or much smaller than the separation between the plates.

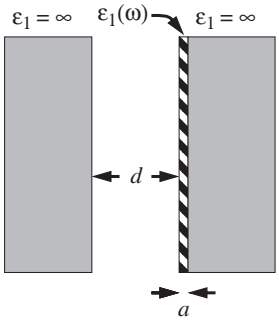


**Figure 4.** Simple geometry for determining the effect of a thin film on a perfectly conducting plate.

### *4.3. Effect of thin films on the plate surfaces*

Either intentionally (Au evaporated onto an Al or Cu coated substrate) or accidentally (formation of oxide layers), every Casimir force measurement has made use of mono- or multilayer coated plates. The calculation of the force for a general film configuration has been given by Spruch and Zhou [67].

A simple geometry that illustrates the effect of a thin material film is shown in figure 4; one of two identical perfectly conducting flat plates is coated with a thin layer (thickness $a$) of a real substance (Au, for example), and the separation between the perfectly conducting surfaces is $d + a$. This simplified problem will allow determination of the qualitative effect of a thin film.

The techniques outlined in section 2.1 can be applied directly to this case. However, in this case, there are some extra boundary conditions.

In general, there are now three wavevectors,

$$K_i^2 = k^2 - \epsilon(\omega)\frac{\omega^2}{c^2}, \tag{38}$$

where $k$ is a real number and $i = 0, 1, 2$, with 0 ($\epsilon_0(\omega) = 1$) representing the space between the plates and 2 ($\epsilon_2(\omega) = \infty$) the perfect conductor, with the requirement that $\mathrm{Re}(K_i) \geqslant 0$, and $\epsilon_1$ can be complex.

As before, there are two type of solution to the wave equation, one with the electric vector parallel to the surfaces (with arbitrary orientation, chosen here as the $y$ axis), $e_y(z)$, and one with the electric vector perpendicular to the surfaces (along the $z$ axis), $e_z(z)$. The wave equation is

$$\frac{\mathrm{d}}{\mathrm{d}z}e_{y,z}(z) - K_i^2 e_{y,z}(z) = 0 \tag{39}$$

and the boundary condition for $e_z$ is that $\mathrm{d}e_z/\mathrm{d}z$ and $\epsilon e_z$ be continuous, while for $e_y$ it is that $\mathrm{d}e_y/\mathrm{d}z$ and $e_y$ be continuous (at the conducting surfaces, $e_y = 0$ and $\mathrm{d}e_z/\mathrm{d}z = 0$). Ignoring unphysical exponentially growing solutions, the solutions are

$$\begin{aligned}
e_{y,z}(z) &= A(\mathrm{e}^{K_0 z} \mp \mathrm{e}^{-K_0 z}) && 0 \leqslant z \leqslant d - a,\\
&= B\mathrm{e}^{K_1 z} + C\mathrm{e}^{-K_1 z} && d - a \leqslant z \leqslant d,\\
\frac{\mathrm{d}e_z}{\mathrm{d}z} &= 0 && z = d,\\
e_y &= 0 && z = d,
\end{aligned} \tag{40}$$

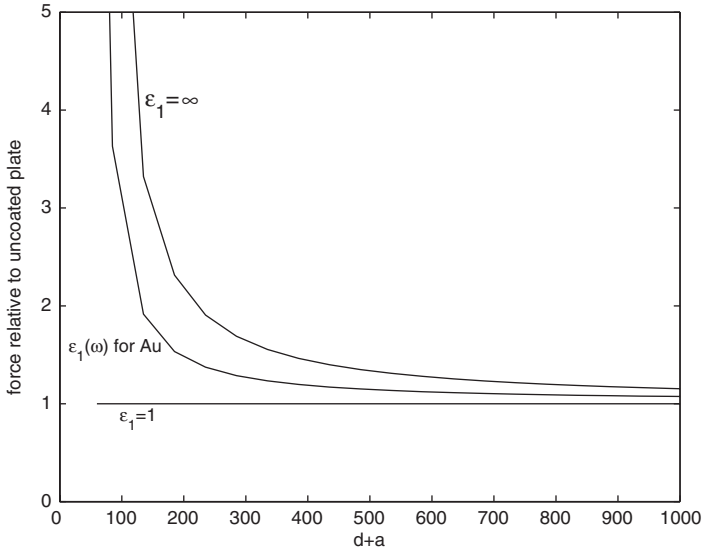


**Figure 5.** The numercially calculated effect of a 35 nm thick Au film on a perfectly conducting surface. Lower curve, no coating; middle curve, Au film; upper curve, perfectly conducting film. The Au film effect is of the order of 50% of the perfectly conducting film effect in the 100–200 nm range.

where the $\mp$ sets $e_y = 0$ or $\mathrm{d}e_z/\mathrm{d}z = 0$ at the conducting boundary located at $z = 0$. Thus, there are two sets of linear equations involving $A$, $B$ and $C$ for the two cases. The condition for non-trivial solutions of these equations is that the determinant of the coefficient matrix be zero, yielding the following two expressions:

$$f_y(\omega, k, d) = 0 = \frac{[(\mathrm{e}^{2K_1 a} + 1)K_1 + (\mathrm{e}^{2K_1 a} - 1)K_0]}{[(\mathrm{e}^{2K_1 a} + 1)K_1 - (\mathrm{e}^{2K_1 a} - 1)K_0]}\mathrm{e}^{2K_0 d} - 1, \tag{41}$$

$$f_z(\omega, k, d) = 0 = \frac{[(\mathrm{e}^{2K_1 a} - 1)K_1 + \epsilon_1(\omega)(\mathrm{e}^{2K_1 a} + 1)K_0]}{[(1 - \mathrm{e}^{2K_1 a})K_1 + \epsilon_1(\omega)(\mathrm{e}^{2K_1 a} + 1)K_0]}\mathrm{e}^{2K_0 d} - 1. \tag{42}$$

$F(d)$ for an Au film 35 nm thick is shown in figure 5; $\epsilon_1(\mathrm{i}\xi)$ was determined from tabulated optical constants as described in [60].

## 5. Finite temperature correction

The Casimir force for finite temperatures has also received much attention. In the high-temperature limit, equation (4) does not contain $\hbar$. In this limit the Casimir force is analogous to the Rayleigh–Jeans black-body spectrum. This also can be seen from the following argument. For a photon gas, the radiation energy, $E$, is simply related to the free energy, $F$, by $E = -3F$. In the long-wavelength limit, the spectral energy in a volume, $V$, is given by (see section 63 of [24])

$$\mathrm{d}E_\omega = \frac{VkT}{\pi^2 c^3}\omega^2\,\mathrm{d}\omega, \tag{43}$$

which is the Rayleigh–Jeans formula. This formula is an apt description of the free energy spectral density that generates the pressure in the high-temperature limit, assuming $\mathrm{d}F_\omega = -\frac{1}{3}\mathrm{d}E_\omega$.

The pressure is related to the free energy by

$$P = -\left(\frac{\partial F}{\partial V}\right)_T = \left[-d\frac{\partial F}{\partial d} - F\right] V^{-1}, \tag{44}$$

where $V = dA$, $d$ is the plate separation and $A$ is the plate area. The net pressure on a plate is given by the difference in the free energy of the plates as compared with that outside:

$$F_{\text{out}} - F_{\text{in}} = -\frac{1}{3}\int_0^{\omega_{\min}} \mathrm{d}F_\omega = \frac{VkT}{9\pi^2 c^3}\omega_{\min}^3, \tag{45}$$

where $\omega_{\min}$ is the minimum effective frequency (longest wavelength) that satisfies the boundary conditions. By dimensional arguments,

$$\omega_{\min} = \frac{\alpha c\pi}{d}, \tag{46}$$

where $\alpha$ is a numerical constant of order unity. The pressure is therefore

$$|P| = \frac{2\pi\alpha^3}{9}\frac{T}{d^3}. \tag{47}$$

The $1/d^3$ dependence is also found in more sophisticated calculations based on the Lifshitz formalism, and comparison with those results determines $\alpha \approx 0.6$. The above simple discussion shows that the long-range (or high-temperature) correction to the Casimir force can be fully understood by analogy with the Rayleigh–Jeans limit for the black-body spectrum. Schwinger *et al* [55] have some comments on the original Lifshitz calculation of the temperature correction and its validity. Compelling calculations of the finite-temperature correction have been given (e.g. [68]).

### *5.1. Contribution of the* TE *electromagnetic mode*

A recent paper [69], in which simultaneous consideration of the thermal and finite conductivity corrections to the Casimir force between metal plates leads to a significant deviation from experimental results [70, 71] and previous theoretical work, has attracted much interest. The principal conclusion in [69] leading to this discrepancy is that the *TE* electromagnetic mode (***E*** parallel to the surface) does not contribute to the force at finite temperature. Arguments against the analysis given in [69] have been numerous [72–75] but not universally accepted [76, 77].

The assertion in [69] is that at a finite temperature the mode excitation function goes from

$$\frac{1}{2} \to \frac{1}{2}\coth\frac{\hbar\omega}{2kT}, \tag{48}$$

and this function has poles at $\mathrm{i}\hbar\xi/2kt = n\pi$ and the integral over $\xi$ in equation (22) becomes a sum over the residues of the integrand. A dominant contribution to this sum comes from the $n = 0$ term, so the limiting forms of $g_y$ and $g_x$ as $\omega \to 0$ are required. In particular, as $\omega \to 0$, for good conductors $\epsilon \propto \mathrm{i}/\omega$, and by equation (13) $K_0 \approx k$. Therefore $g_y$ diverges as can be seen from equation (17). Since the contribution to the force is $1/g_y$, it has no contribution for $\omega \to 0$.

A careful numerical analysis of the problem shows that the results presented in [69] are mathematically correct. An aspect of the problem that has not been considered in detail is the appropriateness of a dielectric model of the metallic plates at low frequencies, which, as will be shown here, are most relevant for the thermal correction. The purpose of this discussion is to expand on previous work [78] and apply more realistic boundary conditions to this problem, and to show that the experimental results [70, 71] can be fully explained by this application.

The analysis in [79] employs the use of the surface impedance of a metal surface which relates $\boldsymbol{E}_\parallel = \zeta(\omega)\hat{n} \times \boldsymbol{H}_\parallel$. As discussed in [15], section 67, $\zeta(\omega)$ when regarded as a function

of the complex variable $\omega$ has many properties analogous to $\epsilon(\omega)$. As will be shown below, the values of $\omega$ that contribute to the thermal correction described in [69] are in a region where the dielectric boundary conditions are not applicable. It is no longer possible to describe the Casimir force as the integral of an analytic function because one must switch between boundary conditions in different regions of the integral. On the other hand, working with $\zeta(\omega)$ allows the force to be written as an single analytic function on the complex $\omega$ plane for all $\omega$.

### *5.2. Spectrum of the* TE *mode thermal correction of the Casimir force*

Following Ford [80], the spectrum of the Casimir force is given by equations (2.3) and (2.4) of Lifshitz's seminal paper [12]. Note that

$$\frac{1}{2}\coth\frac{\hbar\omega}{2kT} = \frac{1}{2} + \frac{1}{\exp(\hbar\omega/kT)-1} = \frac{1}{2} + g(\omega) \tag{49}$$

and only the second term on the right-hand side is included in the determination of the spectrum of the thermal correction. From equation (2.4) of [12], the spectrum of the *TE* mode excitation between parallel plates can be described by (see also section 3.1 of this report)

$$\left[\frac{\hbar}{\pi^2c^3}\right]F_\omega = \left[\frac{\hbar}{\pi^2c^3}\right]\omega^3 g(\omega)\,\mathrm{Re}\int_C p^2\,\mathrm{d}p\left[\frac{(s+p)^2}{(s-p)^2}\mathrm{e}^{-2\mathrm{i}p\omega d/c}-1\right]^{-1}, \tag{50}$$

$$s = \sqrt{\epsilon(\omega)-1+p^2}, \tag{51}$$

where $d$ is the plate separation, and it has been assumed that the plates are made of the same material with vacuum between them. The integration path, $C$, can be separated into $C_1$ for $p = 1$ to 0, which describes the effect of plane waves, and $C_2$ with pure imaginary values $p = \mathrm{i}0$ to $\mathrm{i}\infty$ for exponentially damped (evanescent) waves.

In anticipation that the effect is a low-frequency phenomenon, the parameters for Au in [69] for Im $\epsilon = \epsilon''$ together with the Kramers–Kronig relations can be used to determine Re $\epsilon = \epsilon'$. For frequencies $\omega < 10^{14}\,\mathrm{s}^{-1}$, to good approximation,

$$\epsilon' = \frac{-1.48\times10^4}{1+(\omega/\omega_0)^2}, \qquad \epsilon'' = \frac{1.8\times10^{18}}{\omega(1+(\omega/\omega_0)^2)} \tag{52}$$

with $\omega_0 = 3.3\times10^{13}\,\mathrm{s}^{-1}$.

In [69], a net deviation from the zero-temperature value of the Casimir force is predicted to be about 25% for a plate separation of 1 $\mu$m at 300 K. The experimental results reported in [70] had their greatest sensitivity around 1 $\mu$m, and disagree significantly with the results in [69]. As a comparison, a numerical integration of equation (50) for $d = 1\,\mu$m and $T = 300\,\mathrm{K}$, using equation (52) for the permittivity, can be performed. The results are shown in figure 6, where the results from the two integration paths are separated. In figure 6(*a*), it can be seen that there is no significant deviation from the perfectly conducting case. On the other hand, the contribution from evanescent waves, shown in figure 6(*b*), is large and the integrated value is in good agreement with the result given in [69].

It can be seen immediately that the main contributions of the *TE*-mode finite conductivity correction are around $\omega = 10^{10}$–$10^{13}\,\mathrm{s}^{-1}$. This behaviour is due to an approximately quadratic increase with $\omega$ of the $C_2$ integral and a suppression beginning at $\omega = kT/\hbar = 4\times10^{13}\,\mathrm{s}^{-1}$ because of the $g(\omega)$ factor. This is a low-frequency range, and certain assumptions in [69] and in the Lifshitz calculation, among others, can be questioned with regard to theoretical predictions relevant to the experimental arrangement in [70].

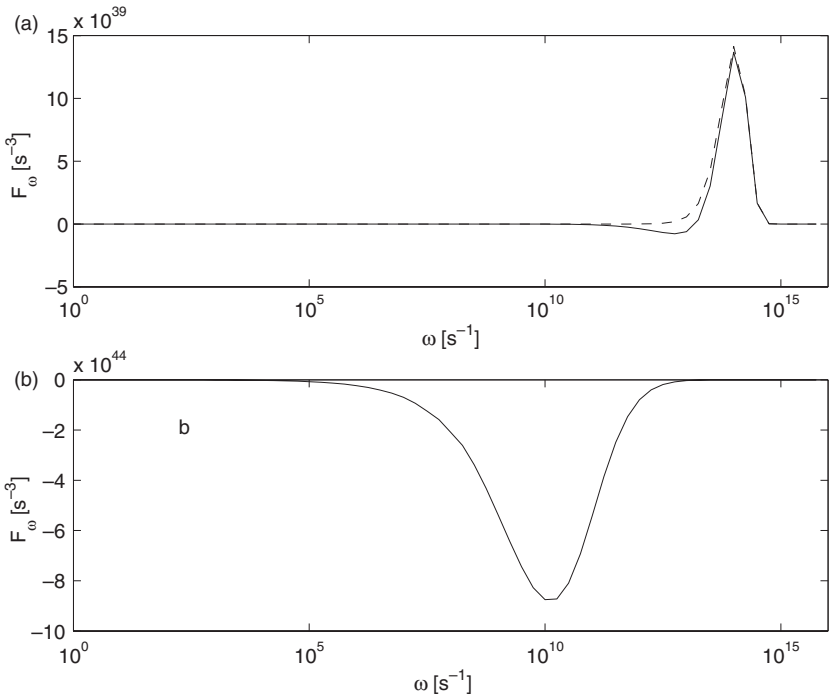


**Figure 6.** The net finite-temperature contribution to the Casimir force is determined by $F = (\hbar/\pi c^3)\int_0^\infty F_\omega \, \mathrm{d}\omega$ and is attractive when $F > 0$. (*a*) The two curves represent the $C_1$ path for perfectly conducting plates (- - - -) and for plates with the permittivity given by equation (52) (——). The net force force for the latter is 0.95 times the perfectly conducting case. (*b*) For a perfect conductor, the $C_2$ integral is zero. The net contribution from the $C_2$ path is $-169$ times the perfectly conducting contribution from the $C_1$ path, and its addition to the *TE* mode zero-point contribution reduces the net *TE* mode force to nearly zero, which is the result obtained in [69]. All are for $d = 1\,\mu$m, $T = 300$ K.

### *5.3. Low-frequency limit and field behaviour in metallic materials*

When the depth of penetration of the electromagnetic field into a metal

$$\delta = \frac{c}{\sqrt{2\pi\mu\sigma\omega}}, \tag{53}$$

where $\sigma$ is the conductivity and $\mu$ is the permeability (for Au and Cu, $\sigma \approx 3 \times 10^{17}\,\mathrm{s}^{-1}$, $\mu = 1$), becomes of the same order as the mean free path of the conduction electrons, it is no longer possible to describe the field in terms of a dielectric permeability [23, 81] because there are non-local correlations in the material and it is not possible to describe the propagation of fields in the material using a simple wavevector derived from a simple dielectric response. This occurs for optical frequencies below $\omega \approx 5 \times 10^{13}\,\mathrm{s}^{-1}$ for metals such as Au and Cu, where the mean free path, at 300 K, is about $3 \times 10^{-6}$ cm [82] (p 259). At frequencies above $10^{14}\,\mathrm{s}^{-1}$ the permeability description again becomes valid because on absorbing a photon, a conduction electron acquires a large kinetic energy and has a shortened mean free path. However, in the interaction of a field with a material surface, $\boldsymbol{E}$ and $\boldsymbol{H}$ can be related linearly through the surface impedance (which relates the electric field at the surface to a surface current and hence magnetic field); this approach has been used in calculation of the Casimir force [79]. Another approach is to perform a microscopic calculation of the noise current as described in [44] and use that with the Lifshitz technique.

It is tempting to interpret the form of the TM and TE modes as described by equations (17) and (18) in terms of reflection coefficients. However, on forming characteristic functions along the lines of equations (16) and (17), using the boundary condition that $\boldsymbol{E}_\parallel = \zeta \hat{n} \times \boldsymbol{H}_\parallel$, where $\zeta$ is the surface impedance and $\hat{n}$ is the surface normal (section 67 of [15]), the perfectly conducting characteristic function results trivially when $\boldsymbol{E}$ and $\boldsymbol{H}$ are related through the surface impedance and the waveguide equations (equations (71.4) of [15]). This treatment is not sufficient for specifying the evanescent surface modes at the material surface, and the method outlined in [79] must be employed.

A correction due to correlated electron motion also arises from the the plasmon interaction with the surface which becomes significant near the plasma frequency of the metal. This correction has been estimated as nearly 10% [45] for sub-micrometre plate separations.

The proper boundary conditions for a conducting plane have been discussed by Boyer [83]. He points out that when (using here the notation of [69]) $\omega \ll \eta^2 \rho / 4\pi$, where $\rho$ is the resistivity and $\eta$ is the dissipation, the usual dielectric boundary conditions are not applicable. For Au, using the parameters in [69], this limit is met for $\omega \ll 4 \times 10^{14}\,\mathrm{s}^{-1}$. This corresponds to an optical wavelength of 5 $\mu$m, which implies that for plate separations significantly larger than this, and of course for $\omega \to 0$, the plates must be treated as good conductors.

The boundary conditions for a conducting surface are discussed in [84] (section 8.1). At low frequencies (e.g. where the displacement current can be neglected), a tangential electric field at the surface of a conductor will induce a current $\boldsymbol{j}_\parallel = \sigma \boldsymbol{E}_\parallel$, where $\sigma$ is the conductivity. The presence of the surface current leads to a discontinuity in the normal derivative of $\boldsymbol{H}_\parallel$, and hence a discontinuity in the normal derivative of $\boldsymbol{E}_\parallel$, at the boundary of a conducting surface. These boundary conditions are quite different from the dielectric case where the fields and their derivatives are assumed continuous.

### *5.4. Electromagnetic modes between metallic plates*

Of interest are the modes between two conducting plates separated by a distance $a$. In the limit where the plates are thin films of thickness $>\delta$, the skin depth, it can be assumed that the plates are infinitely thick and the problem is considerably simplified. This is well-satisfied for the conditions of the experiment [70] when $\omega > 10^{11}\,\mathrm{s}^{-1}$, in which case $\delta < 0.7\,\mu$m compared with the film thickness of 1 $\mu$m. Essentially all of the *TE* mode thermal correction comes in the $10^{11}$ and $10^{13}\,\mathrm{s}^{-1}$ range as shown in figure 6.

Taking the $\hat{z}$ axis as perpendicular to the plates, and the mode propagation direction along $\hat{x}$, for the case of *TE* modes (also referred to as $H$ or magnetic modes), $E_x = 0$. The plates surfaces are located at $z = 0$ and $z = d$. For a perfect conductor, $\partial H_z / \partial z = 0$ at the conducting surfaces. A finite conductivity makes this derivative non-zero, and can be estimated from the small electric field $E_y$ that exists at the surface of the plate (see [84], section 8.1 and equation (8.6)),

$$\vec{E}_\parallel = \hat{y} E_y = \sqrt{\frac{\omega}{8\pi\sigma}}(1 - i)\hat{n} \times \vec{H}_\parallel, \tag{54}$$

where $\vec{H}_\parallel = \hat{x} H_x$ and it is assumed that the displacement current in the metal plate can be neglected ($\sigma \gg \omega$) and that the inverse of the mode wavenumber is less than $\delta$.

This approximation is good so long as the effects of the transverse spatial variation are small compared with the damping length in the plate. Specifically, if we impose a field distribution along the surface as $\mathrm{e}^{\mathrm{i}kx}$, this distribution propagates diffusively into the plate. The solutions to the diffusion equation show that the disturbance propagates into the plate as $1/\delta + \mathrm{i}k$. From numerical calculations, the dominant contribution to the Casimir force comes

from $k < 1/4d$, roughly independent of frequency, with the contribution from higher $k$ falling off exponentially. So when $\delta < 4d$ this approximation is extremely good and is satisfied for the experimental situation in [70] for the frequencies of interest for the thermal correction. (For low frequencies, $K_0 \approx k$.)

$E_y$ and $H_x$ are related through Maxwell's equation, $\vec{\nabla} \times \vec{H} = \partial \vec{E}/c\partial t$. Assuming a time dependence of $\mathrm{e}^{-\mathrm{i}\omega t}$, and vacuum between the plates,

$$\frac{\partial H_x}{\partial z} = \pm \frac{\mathrm{i}\omega}{c} E_y, \tag{55}$$

where $\pm$ indicates the sign of $\hat{n}$ at $z = 0$ and $z = a$, respectively. The boundary conditions at the surfaces are thus

$$\frac{\partial}{\partial z} H_z = \pm \mathrm{i} \sqrt{\frac{\omega}{8\pi\sigma}} \left(\frac{\omega}{c}\right) (1 - \mathrm{i}) H_z \equiv \pm \alpha H_z. \tag{56}$$

Solutions of the form $H_\parallel(z) = A\,\mathrm{e}^{Kz} + B\,\mathrm{e}^{-Kz}$, where $K^2 = k^2 - \omega^2/c^2$ and $k$ is the transverse wavenumber, can be constructed for the space between the conducting plates. The eigenvalues, $K$, can be determined by the requirement that equation (55) be satisfied at $z = 0$ and $z = a$. With the usual substitution $\omega = \mathrm{i}\xi$, the eigenvalues, $K$, are then given by (see [12], section 7.2)

$$g_y(\xi, k, d)(\xi) \equiv \frac{(\alpha + K)^2}{(\alpha - K)^2} \mathrm{e}^{2Kd} - 1 = 0 \tag{57}$$

and the force can be calculated by the techniques outlined in section 3.1.

This result can be recast in the notation of the Lifshitz formalism, and the spectrum of the thermal correction can be calculated as before. Noting that $K = \mathrm{i}\omega p/c$,

$$F_\omega = \omega^3 g(\omega) \int_C p^2 \mathrm{d}p \left[ \frac{(\alpha + \mathrm{i}\omega p/c)^2}{(\alpha - \mathrm{i}\omega p/c)^2} \mathrm{e}^{-2\mathrm{i}\omega p d/c} - 1 \right]^{-1}. \tag{58}$$

Results of a numerical integration are shown in figure 7, where it can be seen by comparison with figure 6 that the metallic plate boundary condition does not show a significant contribution from the $C_2$ integral of the *TE*-mode thermal correction and is therefore similar to that for the 'perfect conductor' boundary condition. This reconciles the discrepancy between the prediction in [69] and the experimental results reported in [70].

The problem of calculating the *TE* mode contribution to the Casimir force has been treated previously with the 'Schwinger prescription' [55] of setting the dielectric constant to infinity before setting $\omega = 0$. This prescription has become controversial [3], a term that can be used to describe the entire history of the theory of the temperature correction. However, there is no doubt that the issues brought up in [69] are important.

The purpose of the calculation presented here is to take a different approach and to study the low-frequency behaviour of the correction in order to understand its character, and to show that the finite temperature correction in [69] is a low-frequency phenomenon. The frequency is sufficiently low for treating the plates as bulk dielectrics to be not valid. By use of a more realistic description of the field interaction with the plates, it was shown that the modes between metallic plates of finite conductivity produce a finite temperature correction in good agreement with the perfectly conducting case. The principal difference between this result and the previous work is that the possibility of the derivatives of the fields at the conducting boundary being discontinuous is allowed. This possibility exists because the fields produce currents in the conducting plates that are discontinuous across the boundary between the vacuum and the conductor. Although it is tempting to model the finite conductivity as a modification of the dielectric permittivity, such a model fails when the mean free path of the conduction electrons exceeds the penetration depth of the electromagnetic field, and thus fails for frequencies of interest for the thermal correction to the *TE* electromagnetic mode.

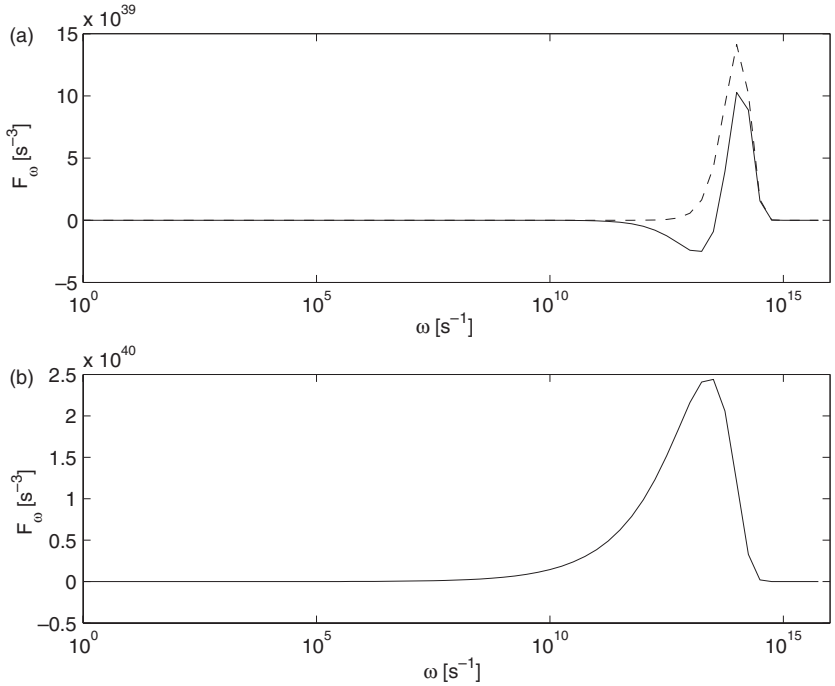


**Figure 7.** Numerical results for $F_\omega$ using the finite conductivity boundary conditions. The integrated force for the $C_2$ path contribution is 1.47 times greater than the $C_1$ integration, and the total net force for both paths is 1.75 times greater than the perfectly conducting case. Treatment of the plates as conducting metals fails above $\omega = 10^{14}\,\mathrm{s}^{-1}$. All are for $d = 1\,\mu$m, $T = 300\,$K.

As shown here, the conducting boundary conditions that are applicable for frequencies where the *TE* mode thermal correction has its significant contribution lead to a net increase in the *TE* mode force, and the correction is of the same magnitude as the perfectly conducting case. This result is in agreement with the experimental results reported in [70, 71]. However, additional and improved experiments with large plate separations (greater than $2\,\mu$m) with both conducting and dielectric plates would provide the definitive test. A particularly tempting dielectric would be diamond, which offers both theoretical and experimental benefits. A comparison with lightly doped germanium plates, where $\delta$ (the skin depth) is large, would also provide a test of the theory presented here and would not suffer from spurious effects due to electric charge accumulation.

## 6. Experiments

### *6.1. Overview*

The theoretical work on the Casimir force far outweighs experimental work: perhaps a few dozen experiments have been performed (with the exception of observations of Casimir effects in colloid chemistry which are beyond the scope of this review) compared with the many hundreds of theoretical papers on the subject. This curious situation is due both to the difficulty of the experiments and to the fact that nobody expects a major failure of the basic theory.

The Sparnaay experiment [85] of 1958 is repeatedly quoted as verification of the Casimir force (equation (1)) and appears to be the first to use metal plates; the accuracy of this measurement was such that the exponent of $d$ in equation (1) could be determined to $\pm 1$.

The experimental situation as of 1989 has been reviewed by Sparnaay in the volume prepared in honour of Dr Casimir's 80th birthday [6], and the situation as of 2000 has been reviewed in [7], prepared in honor of Dr Casimir's 90th birthday. Two experiments were performed in the late 1990s, both with significantly better accuracy than had been previously obtained. These two experiments were based on a torsion pendulum balance [70] and on AFM [57]. The work reported in [70] showed that it was possible to obtain high-accuracy results by using modern experimental techniques, and this work started a sort of renaissance in Casimir measurements.

All recent experiments employed techniques that were developed in particular by van Blokland and Overbeek [61] in the measurement of the attractive forces between metallic films. Measurements between metallic films pose difficult problems compared with dielectric films, for which optical techniques can be used for alignment and distance measurements. In the case of metallic films, the distance is determined by measurement of the capacitance between the plates. Alignment is simplified by making one plate convex, in which case the geometry is fully determined by the radius of curvature, $R$, at the point of closest approach, and the distance between the plates, $d$, at that point. This technique was first put forward by Derjaguin [14] and has found broader application as the proximity force theorem [86], which can be understood as follows. Near the point of closest approach, the distance between the plates can be written as

$$d(r) = d + \frac{1}{2R}r^2, \tag{59}$$

where $r$ is the distance from the point of closest approach in the plane tangent to the surfaces at the point of closest approach. The net force is given by the integral of the force per unit area,

$$\mathcal{F}(d) = 2\pi \int_0^\infty F\left(d + \frac{r^2}{2R}\right) r\,\mathrm{d}r = 2\pi \int_d^\infty F(u) R\,\mathrm{d}u = 2\pi \mathrm{R}E(d), \tag{60}$$

where $E(d)$ is the energy per unit area. There is some evidence that this relationship is exact for the Casimir force [35].

For the plane-sphere geometry, equation (1) becomes

$$F(d) = 2\pi R E(d) = 2\pi \frac{\pi^2}{240}\frac{1}{3}\frac{\hbar c R}{d^3}, \tag{61}$$

where $R$ is the radius of curvature and $E(d)$ is the energy per unit area that leads to the force in equation (1). It should be noted that the plate area does not enter into equation (2), but will when the separation is sufficiently large. Most recent experiments employed one convex plate and one flat plate.

Essentially all of the early experiments (before 1980) relied on the use of cantilever balances, and generally produced data such that the $1/d^n$ force law could be determined to roughly 50% accuracy (in $n$), and the change in the nature of the attractive force for very short distances (e.g. where the ultraviolet cutoff in the electric response of the plate material becomes important) could be observed.

The improvements gained in recent experiments are due to the elimination of mechanical hysteresis in the balance, the use of modern piezoelectric transducers to automatically control the plate positions very accurately and the use of computers for automated data collection.

The most recent experiment employed the use of AFM techniques [57]. The force sensitivity of these techniques is not as great as for the torsion pendulum, but the system is more readily and reproducibly controlled. However, the reduced sensitivity limits the maximum measurement separation to small distances where a number of corrections become very large, as has been discussed. It appears that with proper theoretical analysis, the Casimir force law can be tested to a precision better than 1% using this technique.

### *6.2. Torsion pendulum experiment*

In [70], hysteresis was eliminated by using a torsion pendulum. An accuracy better than 10% was achieved, which was much better than expected, but was limited by calibration uncertainties and lack of knowledge of the metallic film properties.

Since the time of Cavendish's measurement (late 18th century) of the gravitational constant, $G$ [20], which in some ways marks the beginning of modern experimental physics, it has been appreciated that the torsion pendulum is one of the most sensitive devices known. A modern version of Cavendish's experiment was developed by Crandall and associates of Reed College [87] which inspired the design used in [70]. However, to obtain greater accuracy and repeatability for the Casimir force measurement, the magnetic feedback used in [87] was replaced by an electrostatic system. The design is different from the horizontal torsion balance used by van Silfhout [88] particularly because the angular force constant, $\alpha$, and the damping constant are at least two orders of magnitude smaller for the hanging pendulum. For short times (a few seconds of averaging) the principal noise source was thermal fluctuations (e.g. Brownian motion); in this time limit, the signal to noise scales as the square-root of the mechanical dissipation constant of the pendulum [89]. For longer averaging times, vibration and tilt of the apparatus were the dominant noise sources.

The torsion pendulum experiment was rather unwieldy in that the torsion pendulum was over 60 cm in length, and was therefore prone to such subtle effects as the weight of the experimenter distorting a concrete floor, resulting in a slight tilting of the apparatus and thereby spoiling the careful alignment. These sorts of effects were eventually controlled, but achieving better than 5% accuracy with this technique would seem difficult.

In hindsight, it is remarkable that the torsion balance experiment, which was intended as a demonstration, worked as well as it did. The improvement over previous measurements is due to a number of factors, including the high sensitivity of the hanging torsion pendulum and its lack of mechanical hysteresis, larger measurement distances so that vibration and mechanical instabilities were less important, improved piezoelectric transducers and automated data collection so that large amounts of data could be analysed and averaged.

Much improvement over the present accuracy obtained by this technique is unlikely. The apparatus was rather unwieldy with its enormous vacuum can and its susceptibility to tilt. The length of the torsion fibre might be significantly shortened, reducing both the intrinsic sensitivity (bad) and the sensitivity to external perturbations (good); however, we must bear in mind that a factor of 10 improvement in sensitivity only extends the measurement distance by a factor of about 2. At present, a high-sensitivity torsion pendulum is being designed at Los Alamos, with the intent of addressing the finite temperature corrections. The theory can be vigorously tested by measurements between dielectric plates (diamond), semiconducting plates (n-doped Ge with 40 $\Omega$ cm resistivity) and gold-coated copper [89].

### *6.3. AFM experiments and MEMs*

In his 1989 review [6], Sparnaay discusses the possibility of using AFM to measure the Casimir force; AFM had just been invented at that time [90]. It was not until late 1998 that results from an AFM Casimir experiment were reported by Mohideen and Roy [57].

In this experiment, an Au/Pd+Al coated, 0.3 mm polystyrene sphere is attached to an AFM cantilever. A similarly coated optically polished sapphire plate was attached to a piezoelectric transducer and brought near the sphere. The attractive force was determined by reflecting a laser beam from the cantilever tip; the displacement of the laser beam on a pair of photodiodes produced a difference signal proportional to the cantilever bending angle.

The sensitivity of the apparatus was such that the absolute force could be determined with a fractional error of 1% at $d = 100$ nm, and about 100% at 900 nm.

The use of AFM to measure the Casimir force has been a real breakthrough; this is because the AFM technique is very stable and reproducible. Unfortunately, it is limited to measurements of short distances where there are significant theoretical uncertainties in the interpretation of the data. For the first time testing equation (1) or its modification for real materials to better than 1% accuracy appears possible. As described in [57], it was anticipated that a factor of 1000 improvement in sensitivity appears possible, which would extend the separation where the Casimir force can be measured to 1% accuracy to about 1 $\mu$m. At this distance, the theoretical uncertainties associated with the corrections for real materials, as described previously, become much less important. Progress towards improved accuaracy has been rapid [91].

The fundamental differences between AFMs and microelectromechanical machines (MEMs) are not obvious. The practical difference is that MEMs tend to be fabricated entirely on a substrate (e.g. silicon wafer). One of the first reports of an effect of the Casimir force in a MEMs system is in [92], where, when a critical voltage was applied to the system, the cantilever would irreversibly stick due to the Casimir force as discussed in [93]. MEMs techniques were developed to a high level by Chan and collaborators at Bell Laboratories [94, 95], who have set the accuracy standard in the field by use of microelectromechanical torsion oscillators (MTOs) where the Casimir force is detected and measured by its non-linear distance dependence which causes a change in MTO resonant frequency, or by deflections of an oscillator through the unbalancing of a capacitive bridge. A typical $Q$ for an MTO is around 10 000.

In the experiments described in [71], the MTO frequency was about 700 Hz. The MTO was used in both the dynamic (measurement of oscillator frequency) and static (deflection of cantilever capacitively measured) modes. The sensitivity was around 1.4 pN $\mathrm{Hz}^{-1/2}$, with one plate in the form of a ball with radius of curvature between 0.1 and 0.6 mm. This allowed measuring the force with sufficient accuracy to test the finite temperature effect described in [15] which is not supported by data. The results of these experiments were used to limit the strength and magnitude of new Yukawa-type forces, as described in section 7.4. In [96] the force between dissimilar metals was measured using similar techniques. In this instance, there was difficulty in obtaining agreement at the per cent level with theory, and although the deviation is in the same direction as the prediction in [15], the deviation is too small to be attributed to that source alone. The authors conclude that the errors are due to imperfect knowledge of the optical properties of the plates.

Using AFM and MEMs techniques, the force between *flat* plates has been measured with 15% precision in the 0.5–3.0 $\mu$m range [97]. The area over which the Casmir force was measured was 1.2 mm by 1.2 mm. One of the outstanding requirements in such a measurement is the parallelism of the plates. Dust and dirt were removed from the surfaces by use of an in-vacuum cleaning tool operated under inspection using a scanning electron microscope (SEM). The SEM was also used to initially set the parallelism of the plates, with the final alignment done by maximizing the capacitance between the plates at the minimum separation.

The most recently reported Casimir force measurement was between a gold-coated plate and a sphere coated with a hydrogen-switchable mirror (HSM) using a MEMs techniques [98]. The HSMs are shiny metallic mirrors that become transparent on hydrogenation. The effect is reversible. Unfortunately, despite the marked change in the reflective properties of the HSM, no change in force was seen upon hydrogenation. This is partly due to the fact that the dielectric properties of the mirror probably do not change much in the infrared region which corresponds to the modes that contribute the most to the Casimir force. In addition, the HSM was covered with a 100 Å layer of Pd. As described in section 4.3, even a thin metallic layer can dominate the characteristics of the force.

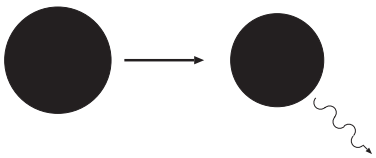

**Figure 8.** Picture of a radiating black hole. The energy taken away by a photon results in a slight shrinkage of the black hole.

## 7. Applications

In his 1948 paper, Casimir made a truly startling discovery that zero-point fluctuations can lead to physical effects on a macroscopic system. This idea has been applied to a great number of fields, in particular quantum chromodynamics (see, e.g. [3]). Casimir's calculational technique has even found a maritime application in determination of the attractive force between two ships in a rough sea owing to modification of the wave structure in the region between the ships [99]. In this section a few surprising applications, primarily with regard to electromagnetic effects, will be discussed.

In the realm of nanotechnology, the forces between the components of a mechanical system can be easily dominated by the Casimir force. It is unclear whether the Casimir force will be, in general, a nuisance or a useful feature in the nanoengineering world. This is because the force is very non-linear. One could imagine weakly coupling mechanical oscillators using the Casimir force. At the time of writing this, the nanoengineering uses remain speculative. The use of magnetic materials to produce a repulsive Casimir force, which would eliminate stiction, is discussed in [52], but it is unclear whether a material with a sufficient magnetic response at optical frequencies can be identified [53, 54].

### *7.1. Hawking radiation and the dynamical Casimir effect*

The idea put forward by Hawking that black holes can 'evaporate' [100, 101] led to the more general notion that an accelerated frame appears bathed in a thermal field (the 'Unruh effect' [102, 103]) with temperature

$$T = \frac{\hbar a}{2\pi kc}, \tag{62}$$

where $a$ is the acceleration, $k$ is Boltzmann's constant and $c$ is the velocity of light. The acceleration promotes zero-point fluctuations, observed from the accelerating frame, to thermal fluctuations that follow a black-body spectrum.

Hawking's idea is illustrated in figure 8; if the boundary of a black hole fluctuates, a photon pair can be created. If one photon escapes, the black hole loses energy and shrinks slightly. The inverse process is very unlikely.

The 'Hawking Temperature' of a black hole can be instantly calculated (in a non-rigorous fashion) from equation (62). If we set $a$ as the acceleration at the Schwarzshild radius of a black hole,

$$r_s = \frac{2GM}{c^2}, \qquad a = \frac{GM}{R_0^2} = \frac{c^4}{4GM} \Rightarrow T = \frac{\hbar c^3}{8\pi k}, \tag{63}$$

which is precisely Hawking's result.

Based on the equivalence principle, it is tempting to assign a temperature to any object at rest (relative to the source) in a gravitational field, e.g. an atom on the Earth's surface, as a

number of authors have asserted [104]. However, a finite temperature in this situation, which would necessarily lead to the radiation of electromagnetic energy, would violate conservation of energy. Black holes can radiate because the radius can shrink with the emission of a photon.

The first crucial point in the analysis of radiation of an at-rest object is that the gravitation field couples equally to all forms of mass–energy. This is closely related to the classical electromagnetism result that a particle undergoing hyperbolic motion (i.e. unconstrained motion in a gravitational potential) does not radiate, as first suggested by Pauli. This is regarded as one of the surprising results of modern physics, and Peierls [105] has a lucid discussion of the relevant issues for the classical problem. For the quantum case, the answer is simple: radiation from atoms is stimulated by the zero-point field, and in any local frame, the atoms and local zero-point field are subject to the same acceleration. In the derivation of equation (62) it is assumed that the acceleration is relative to a rest frame that contains the zero-point fluctuations. So the second crucial point is that there is no relative acceleration between the zero-point field and the atoms in a local frame, and hence no temperature differential.

Questions regarding Mach's principle are also of interest. If we imagine an accelerated observer in an otherwise empty universe, what temperature would we assign? The answer is that in order to maintain a steady acceleration, matter or energy would have to be ejected from the accelerated observer's frame. This ejected material would not be subject to external forces, and would thus provide an observable (eventually!) reference frame, and hence the acceleration would be evident.

The Unruh effect is closely related to the dynamical Casimir effect, where photons are generated when the plates of a Casimir experiment are accelerated. The possibility that sonoluminescence is due to such a process, as first suggested by Schwinger [106], has received much attention, but has largely been ruled out, in particular by Brevik *et al* [107]. A splendid review of the dynamical Casimir effect in this context is provided in Milton's book [3]. It has now been essentially proven that sonoluminescence is due to high-speed jets formed due to, for example, Rayleigh–Taylor instabilities when cavitation bubbles collapse [108–110].

Milonni provides one of the most lucid derivations of the Unruh effect ([5], section 2.10). He shows that the electromagnetic field correlation function of a zero-point field as observed by an observer undergoing proper acceleration is the same as a black-body field with temperature given by equation (62). One interesting result is that the zero-point field correlation function between inertial frames in relative motion is

$$\langle \phi(\vec{y}, t), \phi(\vec{y} + \vec{x}, t + \tau) \rangle = \frac{\hbar c}{\pi} \frac{1}{x^2 - c^2\tau^2} \tag{64}$$

and is an invariant. This is directly applicable to the radiation and Mach's principle questions previously discussed.

*7.1.1. Simple model of Unruh effect.* In order to obtain an elementary understanding of the origin of the Unruh effect, we can consider a simplified system to analyse the effects of relative acceleration. Shown in figure 9 are two frames, one containing a single harmonic oscillator accelerated relative to a frame containing many distinct-frequency but weakly-coupled oscillators at $T = 0$. If a single phonon of frequency $\omega$ is transferred (by an unspecified process) from the accelerated frame to a resonant oscillator in the rest frame, in a time $1/\gamma$ (assume $\langle n \rangle$, harmonic oscillator quantum number, is small for both oscillators), it will be transferred back after an additional time $1/\gamma$. Now during this time, the accelerating frame undergoes a time dilation relative to the non-accelerated frame given by

$$\frac{\mathrm{d}t}{\mathrm{d}\tau} = \left(1 + \left(\frac{a\tau}{c}\right)^2\right)^{1/2} \approx 1 + \frac{1}{2}\left(\frac{a\tau}{c\gamma}\right)^2, \tag{65}$$

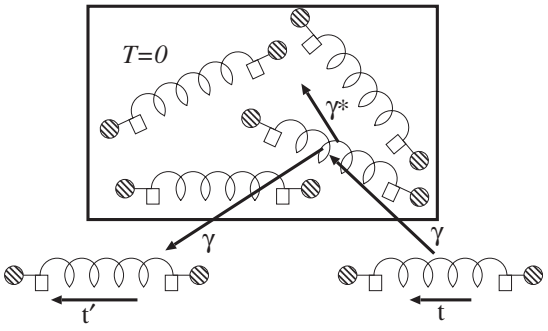


**Figure 9.** Simple model to show the effects of relative acceleration.

and so during this time, the resonance frequency of the oscillator in the accelerating frame changes by

$$\delta\omega = \frac{\mathrm{d}\tau}{\mathrm{d}t}\omega - \omega = -\frac{\omega}{2}\left(\frac{a\tau}{c\gamma}\right)^2. \tag{66}$$

Assuming the harmonic oscillators in the rest frame are very broad, the probability of emitting a phonon at $\omega - \delta\omega$ is essentially the same as that for $\omega$. Taking into account the fact that a phonon can be lost to the 'bath' in the rest frame, the apparent rate of energy flow from the accelerating frame to the rest frame is

$$\gamma\left(\frac{\gamma}{\gamma^* + \gamma}\right)\frac{\hbar\omega}{2}\left(\frac{a}{c\gamma}\right)^2 = \frac{1}{1/Q + 1/Q^*}\left(\frac{a}{c}\right)^2 = \dot{E} = \gamma kT, \tag{67}$$

where $Q = \omega/\gamma$, $Q^* = \omega/\gamma^*$. Thus the accelerated frame appears to be at a finite temperature, which, in this case, is proportional to $a^2$ and depends on the phonon exchange rate. We have not assumed that there is a zero-point motion, but only that the harmonic oscillators are quantized.

Thus, given that harmonic systems in an accelerated frame appear to be at a finite temperature, the existence of the Unruh effect is not surprising. However its specific calculation is nontrivial.

### *7.2. Marconi's coherer*

The first detector for radiated electromagnetic waves was the 'coherer' invented by David Edward Hughes (1830–1900), who was first to demonstrate the transmission of electromagnetic waves, seven years before Hertz's experiments [111]. Hughes was able to detect signals from a spark transmitter at a distance of 500 yards, using a microphone contact (later referred to as a 'coherer'). He correctly claimed that the signals were transmitted by electric waves in the air. Hughes did not publish his work until much later because after demonstrating the effect, the leading observers were not convinced that the effects were not due to ordinary electromagnetic induction. (Joseph Henry observed effects that were likely due to electric waves as early as 1842.)

Hughes' coherer as a detector was further developed by Branley, Lodge, Popov and into its highest engineering form by Marconi, as shown in figure 10. It is in fact easy to demonstrate the coherer effect. If two wire leads are inserted into opposite sides of a small cup of metal filings, the effective resistance suddenly drops, by as much as a factor of 100, when a critical voltage is applied across the leads. The applied voltage can be of either alternating or direct current, and for leads placed a few millimetres apart with filing sizes of the order, 0.1 mm,

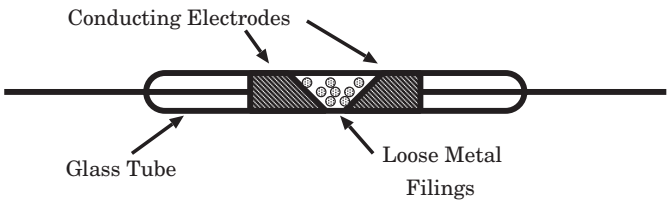


**Figure 10.** Schematic of the coherer detector as developed by Marconi.

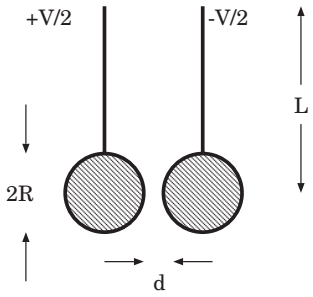


**Figure 11.** Simple model of the metallic particles in a coherer.

the critical voltage is about 3 V. The coherer is an effective but not sensitive detector of radio signals and was superseded by more effective detectors in the early 20th century.

It has been generally assumed that the coherer action is due to the metal filings 'welding' together in the presence of infinitesimal sparks that occur between the filings when a voltage is applied. However, a more likely explanation is that the filings, which are loosely packed, coated with oxide and probably dirty, are initially separated enough that current flow occurs as a percolation process. When a voltage is applied, the particles attract mutually, pulling the particles together. When the separation is small enough, the Casimir force takes over and the filings stick together, creating a semi-permanent low-resistance path through the filings that persists even when the voltage is removed. Shaking or vibrating the coherer restores the coherer to the high-resistance state.

The foregoing picture can be developed into a model, schematically shown in figure 11. Two metal spheres of radius $R$, separated by a distance $d$, with voltage $V$ applied between them, will be mutually attracted. A restoring force in this picture is due to gravity, the two spheres being supported as pendulums hanging from conducting strings of effective length $L$.

The force between the spheres is easy to calculate from the proximity force theorem and the energy between parallel capacitor plates of area $A$,

$$F(d) = 2\pi R\frac{E(d)}{A} = \frac{\pi\epsilon_0}{d}V^2. \tag{68}$$

The spheres will pull together when the derivative of the electric force exceeds the derivative of the restoring force, $mg\delta d/L$, where $m = 4\rho\pi R^3/3$ is the mass of the spheres, $\rho$ is the density of the filings and $\delta d$ is the deviation from the initial separation. From the second derivative,

$$\frac{\pi\epsilon_0 R}{(d-\delta d_c)^2}V_c^2 = \frac{mg}{L}, \tag{69}$$

where $V_c$ is the critical voltage where the derivative are equal. $\delta d_c$ is also determined by

$$\frac{\pi\epsilon_0 R}{(d-\delta d_c)}V_c^2 = \frac{mg\delta d_c}{L} \tag{70}$$

and, surprisingly, the ratio of these two equations determines $\delta d_c = d/2$. Therefore,

$$V_c^2 = \frac{g\rho d^2 R^2}{3\epsilon_0 L}. \tag{71}$$

Taking $R = 0.1\,\text{mm}$, $L = 0.1\,\text{mm}$ (pendulum length the same size as a filing radius), $d = 0.01\,\text{mm}$ determined for Cu ($\rho = 9\,\text{g}\,\text{cm}^{-3}$) implies $V_c \approx 7\,\text{V}$ which is in reasonable agreement with experiment. Exceeding the critical voltage causes the filings to pull together, and they then cohere due to the Casimir force. This is a situation similar to the effect observed in a MEMs experiment where the cantilever became stuck when a critical voltage was exceeded [92], as described in section 6. It is therefore fair to say that the coherer was the first engineered MEMs system.

For Marconi's first transatlantic transmission, a power of $P = 10^5\,\text{W}$ was generated on the Cornwall coast at Poldhu. Messages were received at a distance of $R = 3.5 \times 10^6\,\text{m}$, in Newfoundland. The energy flux, through the Poynting vector and the characteristic impedance of free space, $Z_0 = 377\,\Omega$, can be used to estimate the electric field at that distance, assuming the power flux falls off as the distance squared:

$$\frac{P}{4\pi R^2} = \frac{E^2}{2Z_0} \rightarrow E \approx 10^{-3}\,\text{V}\,\text{m}^{-1} \tag{72}$$

and so with a modest antenna system, the detector might have a 0.01 V signal, neglecting atmospheric absorption which can be significant at the wavelength Marconi used. This voltage is significantly below what one could reasonably expect a coherer to detect, even if it is biased to near the critical voltage. In fact Marconi's first transatlantic signals were detected with a 'mercury coherer' (now known to be effectively a pn junction) developed by the Indian scientist Sir J C Bose. (In the early days of radio, all detectors were referred to as coherers.) This detector would have had sufficient sensitivity to detect a 0.01 V signal. Sadly, Bose was rarely credited for his contributions to the development of modern radio communications. The output of the mercury coherer could not drive Marconi's pen recorder, and so the record of the reception of the first transatlantic transmission (of the letter S by Morse code) exists as a handwritten entry in Marconi's notebook.

### *7.3. Heating by evanescent waves*

The presence of evanescent or non-propagating electromagnetic fields at the surface of bulk materials can lead to observable effects. For example, if two surfaces at different temperatures are close together, the heat flow due to evanescent waves can exceed the heat flow due to propagating black-body radiation [112].

The existence of a fluctuating field outside of a dielectric has been directly observed in studies of the inelastic scattering of low-energy electrons [113]. Heat flow between a heater and a thermophotovoltaic cell placed in submicrometre proximity has been observed in a MEMs system [114].

The material fluctuation considered for the Casimir force (equation (12)) is also the source term for calculating magnetic noise external to material bodies, in particular conductors. This sort of noise is important in biomagnetic measurements [115] and fundamental physics measurements [116] (note missing factor of $\mu$ in the vector potential in [116], making the noise from conducting magnetic materials similar to ordinary conductors).

*7.3.1. Ion trap quantum computing.* Quantum computing using multiple trapped ions that form entangled states though the vibrational quantum states in a Paul radiofrequency trap has been of broad interest. The issues of decoherence due to interactions with the Johnson noise

field external to conductors is discussed in [117], where it is shown that these effects are too small to be of concern because of the narrow effective bandwidth of the mechanical ion oscillator. Henkel and Wilkens [118] consider the problem of an ion very close to a 300 K surface and find that the heating rate can be extremely large when the separation is of the order of a few micronmetres or less, due to interactions with the evanescent fields. Because there is a large gradient in the surface fields, they couple more efficiently to charged particles compared with the case discussed in [117] where the field is essentially homogeneous across the trap, but fluctuating in time.

### *7.4. Tests for new forces in the sub-millimetre range*

Deviations from Newton's law of universal gravitation have always been of interest but have received considerable attention over the last three decades. This attention is due to new theoretical predictions and to reports of experimental anomalies. For example, in the context of string theory, extra compactified dimensions lead to a modification of Newton's law, and in some models the characteristic length scale is at the micrometre level. A recent review by Fischbach and Talmadge [119] indicates that there are no anomalous forces with strength comparable to gravity over the $1–10^{17}$ cm range.

Agreement between experimental measurements of the Casimir force and theoretical predictions can be used to set limits on possible anomalous interactions [120, 121]. Although these limits correspond to forces many times that of gravity, these are nonetheless the best constraints for short-range forces. These types of experiments provide strong motivation for an improved theoretical understanding of the Casimir force. The current best experimental limits, obtained with a MEMs device, are reported in [71].

### *7.5. Dispersion forces: wetting of surfaces*

The question of the wetting of surfaces can be thought of as a generalization of the Casimir force when one of the plates is a liquid. In 1941, Schiff [122] suggested that the formation of films of superfluid helium on the walls of containers is due to the van der Waals attraction between the substrate and the helium atoms. Lifshitz's theory [12] was cast into a more general form by Dzyaloshinskii, Lifshitz and Pitaevskii (DLP) [123] to include interactions between a substrate and a thin liquid film. Measurements of the thickness of liquid helium films are in good agreement with the generalized theory [124]. More recent studies have shown that liquid helium will not wet a caesium film [125] and this has been experimentally demonstrated [126]. This discovery has a practical application as an important technique in low-temperature physics because an evaporated Cs ring interrupts superfluid film flow and eliminates the associated heat load.

In a series of remarkable experiments, it was demonstrated that liquid water does not wet the surface of ice [127, 128], and this is explained by the DLP theory with the known dielectric responses of ice and water [129].

The DLP theory has also been applied to the wetting of water on indium-tin-oxide films on windshields [130] and is but one of the far-reaching applications of the Casimir force.

## 8. Conclusion

The Casimir force remains one of the most amazing predictions in the history of physics. Nearly 50 years after its prediction, it has finally become possible to measure the force with per cent-level accuracy, and theory is now lagging experiment.

The source of zero-point fluctuations has been debated, but the general consensus is there are different, yet equivalent, ways of interpreting the same phenomenon [5]. The idea that boundaries can affect the zero-point fluctuations of a system has had widespread application.

In the last few years, several experiments have been performed to quantify the character of the Casimir force between solid bodies and have shown a new level of accuracy; in particular, the AFM technique offers great promise for testing equation (1) and its modifications for the case of real materials to better than 1% precision. If the sensitivity of the AFM and MEMs-based experiments can be increased substantially, the measurement region can be extended to larger separations where the theoretical uncertainties discussed in this report are substantially reduced. Perhaps even the effect of finite temperature [68] will be measurable in the not-too-distant future, and the veracity of [69] can be tested by repeating the measurements with dielectrics (diamond), semiconductors (lightly doped germanium) and other metals. As discussed in section 5, these materials should all exhibit thermal corrections of different character. At present, this is the outstanding problem in the theory of the Casimir force.

## References


[1] Casimir H B G 1948 *Proc. Kon. Ned. Akad. Wetenschap. Ser.* B **51** 793

[2] Bordag M (ed) 2002 *Fifth Workshop on Quantum Field Theory under the Influence of External Conditions (Leipzig, Germany, 10–14 September 2001) Int. J. Mod. Phys.* A **17** 711–1059

[3] Milton K A 2001 *The Casimir Effect: Physical Manifestations of Zero-Point Energy* (Singapore: World Scientific) p 54

[4] Mostepanenko V M, Trunov N N and Znajek R L (translator) 1997 *The Casimir Effect and its Applications* (New York: Oxford University Press)

[5] Milonni P W 1994 *The Quantum Vacuum* (San Diego, CA: Academic) pp 221–7

[6] Sarlemijn A and Sparnaay M J 1989 *Physics in the Making: Essays on Developments in 20th Century Physics in Honour of H B G Casimir on the Occasion of his 80th Birthday* (Amsterdam: North-Holland) pp 235–46

[7] Babb J F, Milonni P W and Spruch L (ed) 2000 Casimir forces *Commun. Mod. Phys.* **1** 171–378 (Special issue)

[8] Bordag A, Mohideen U and Mostepanenko V M 2001 *Phys. Rep.* **353** 1–205

[9] Lamoreaux S K 1999 *Am. J. Phys.* **67** 850–61

[10] Axilrod B M and Teller E 1943 *J. Chem. Phys.* **11** 299

[11] London F 1930 *Z. Phys.* **63** 245

[12] Lifshitz E M 1956 *Sov. Phys.—JETP* **2** 73–83

[13] Deriagin B V and Abrikosova I I 1957 *Sov. Phys.—JETP* **3** 819

[14] Derjaguin B V 1960 *Sci. Am.* **203** 47–53

[15] Landau L D and Lifshitz E M 1960 *Electrodynamics of Continuous Media* (Oxford: Pergamon) section 67

[16] Lifshitz E M and Pitaevskii L P 1980 *Statistical Physics: Pt. 2* (Oxford: Pergamon) Chapter 13

[17] Barash Yu S and Ginzburg V F 1975 *Sov. Phys.—Usp.* **18** 305–22

[18] Hawking S W 1999 private communication

[19] Phillip Yam 1997 *Sci. Am.* **277** 82–5

[20] Cavendish H 1798 *Phil. Trans.* **17** 469
M H Shamos 1987 *Great Experiments in Physics* (Mineola NY: Dover) (Reprint)

[21] Whittaker E T and Watson G N 1963 *A Course of Modern Analysis* 4th edn (London: Cambridge University Press)

[22] Rytov S M, Kravtsov Yu A and Tartarskii V I 1989 *Principles of Statistical Radiophysics* vol 3 (Berlin: Springer)

[23] Landau L D and Lifshitz E M 1960 *Electrodynamics of Continuous Media* (Oxford: Pergamon) chapter 9. This chapter has been omitted from later editions of this volume (vol 8 of *Course of Theoretical Physics*)

[24] Landau L D and Lifshitz E M 1980 *Statistical Physics* 3rd edn, Pt. 1 (Oxford: Pergamon) Chapter 12

[25] Schwinger J, DeRaad L L Jr and Milton K A 1978 *Ann. Phys.* **115** 1

[26] Milonni P W 1982 *Phys. Rev.* A **25** 1315–27

[27] Mitchell D J, Ninham B W and Richmond P 1972 *Am. J. Phys.* **40** 674–8

[28] Schatten K H 1989 *J. Franklin Inst.* **326** 755–71

[29] Scheel S, Knoell L and Welsh D-G 1998 *Phys. Rev.* A **58** 700–6

[30] Huttner B, Baumberg J J and Barnett S M 1998 *Europhys. Lett.* **16** 177–82

[31] Munitz M K 1957 *Theories of the Universe* (New York: The Free Press)
See the reprint of: Milne E A The fundamental concepts of natural philosophy, 1943–44 *Proc. R. Soc. Edinb.* A **62** 10–24
[32] Longair M S 1984 *Theoretical Concepts in Physics* (Cambridge: Cambridge University Press)
[33] Pauli W 1973 *Pauli Lectures on Physics* vol 4, ed C P Enz (Cambridge, MA: MIT Press) p 115
[34] Enz C P and Thellung A 1960 *Helv. Phys. Acta* **33** 839
[35] Schaden M and Spruch L 2000 *Commun. Mod. Phys.* **5–6** 275–84
[36] Weinberg S 1989 *Rev. Mod. Phys.* **61** 1
[37] Morse P M and Feshbach H 1953 *Methods of Theoretical Physics* vol 1 (New York: McGraw-Hill) p 413
[38] Van Kampen N G, Nijboer B R A and Schram K 1968 *Phys. Lett.* A **26** 307
[39] Boas M L 1983 *Mathematical Methods in the Physical Sciences* (New York: Wiley) p 609
[40] Churchill R V, Brown J W and Verhey R F 1976 *Complex Variables and Applications* (New York: McGraw-Hill) pp 296–301
[41] Barash Yu S and Ginzburg V F 1975 *Sov. Phys.—Usp.* **18** 305
[42] Tomas M S 2002 *Phys. Rev.* A **66** 52103
[43] Raabe C, Knoll L and Welsch D G 2003 *Phys. Rev.* A **68** 33810
[44] Di Stefano O, Savasta S and Girlanda R 2001 *J. Opt.* B **3** 288
[45] Esquivel R, Villarreal C and Mochàn W L 2003 *Phys. Rev.* A **68** 52103
[46] Casimir H B G 1978 *Rev. Roumaine Physique* **23** 723–6
[47] Boyer T H 1968 *Phys. Rev.* **174** 1764–76
[48] Carniglia C K and Mandel L 1971 *Phys. Rev.* D **3** 280–96
[49] Belinfante F J 1987 *Am. J. Phys.* **55** 134–8
[50] Schaden M and Spruch L 1998 *Phys. Rev.* A **58** 935–53
[51] Kleppner D 1990 *Phys. Today* **43** 9–11
[52] Kenneth O, Klich I, Mann A and Revzen M 2002 *Phys. Rev. Lett.* **89** 033001
[53] Iannuzzi D and Capasso F 2003 *Phys. Rev. Lett.* **91** 029101
[54] Kenneth O, Klich I, Mann A and Revzen M 2003 *Phys. Rev. Lett.* **91** 029102
[55] Schwinger J, DeRaad L L Jr and Milton K A 1978 *Ann. Phys. (New York)* **115** 1
[56] Hargreaves C M 1965 *Proc. Kon. Ned. Akad. Wetensh.* **68** B 231–6
[57] Mohideen U and Roy A 1998 *Phys. Rev. Lett.* **81** 4549
[58] Hargreaves C M 1965 *Proc. Kon. Ned. Akad. Wetenshap. Ser.* B **68** 231
[59] Bezerra V B, Klimchitskaya G L and Romero C 1997 *Mod. Phys. Lett.* A **12** 2613
[60] Lamoreaux S K 1999 *Phys. Rev.* A **59** R3149
[61] van Blokland P H G M and Overbeek J T G 1978 *J. Chem. Soc. Faraday Trans.* **74** 2637
[62] Jenkins F A and White H E 1957 *Principles of Optics* (New York: McGraw-Hill) p 523
[63] Bostrom M and Sernelius B E 2000 *Phys. Rev.* A **61** 046101–3
[64] Lambrecht A, Reynaud S (Comment) and Lamoreaux S K (Reply) 2000 *Phys. Rev. Lett.* **84** 5672–3
[65] van Bree J L M J, Poulis J A, Verhaar B J and Schram K 1974 *Physica* **78** 187
[66] Bordag M, Klimchitskaya G L and Mostepanenko V M 1995 *Phys. Lett.* A **200** 95
[67] Zhou F and Spruch L 1995 *Phys. Rev.* A **52** 297
[68] Brown L S and Maclay G J 1969 *Phys. Rev.* **184** 1272–9
[69] Bostrom M and Sernelius Bo E 2000 *Phys. Rev. Lett.* **84** 4757
[70] Lamoreaux S K 1997 *Phys. Rev. Lett.* **78** 5
Lamoreaux S K 1998 *Phys. Rev. Lett.* **81** 4549
[71] Decca R S *et al* 2003 *Phys. Rev.* D **68** 116003
[72] Lamoreaux S K 2001 *Phys. Rev. Lett.* **87** 139101
[73] Bordag M *et al* 2000 *Phys. Rev. Lett.* **85** 503
[74] Klimchitskaya G L 2002 *Int. J. Mod. Phys.* A **17** 751
[75] Genet C, Lambrecht A and Reynaud S 2002 *Int. J. Mod. Phys.* A **17** 761
[76] Sernelius Bo E and Bostrom M 2001 *Phys. Rev. Lett.* **87** 259101
Brevik I, Aarseth J B and Hoye J S 2002 *Phys. Rev.* E **66** 026119
[77] Hoye J S, Brevik I, Aarseth J B and Milton K A 2003 *Phys. Rev.* E **67** 056116
[78] Torgerson J R and Lamoreaux S K *Preprint* quant-ph/0309153
Torgerson J R and Lamoreaux S K 2004 *Phys. Rev.* E at press
[79] Geyer B, Klimchitskaya G L and Mostepanenko V M 2003 *Phys. Rev.* A **67** 062102
[80] Ford L H 1993 *Phys. Rev.* A **48** 2962
[81] London H 1940 *Proc. R. Soc.* A **176** 522

[82] Kittel C H 1971 *Solid State Physics* (New York: Wiley)
[83] Boyer T H 1974 *Phys. Rev.* A **9** 68
[84] Jackson J D 1975 *Classical Electrodynamics* 2nd edn (New York: Wiley)
[85] Sparnaay M J 1958 *Physica* **24** 751–64
[86] Blocki J, Randrup J, Swiatecki W J and Tsang C F 1977 *Ann. Phys.* **105** 427
[87] Crandall R E 1983 *Am. J. Phys.* **51** 367
[88] van Silfhout A 1966 *Proc. Kon. Ned. Acad. Wetensch. Ser.* B **69** 501
[89] Lamoreaux S K and Buttler W T 2004 *Preprint* quant-ph/0408027
[90] Binnig G, Quate C F and Gerber Ch 1986 *Phys. Rev. Lett.* **56** 930
[91] Chen F, Harris B W, Roy A and Mohideen U 2002 *Int. J. Mod. Phys.* A **17** 711–21
[92] Buks E and Roukes M L 2001 *Europhys. Lett.* **54** 220–6
[93] Serry F M, Walliser A D and Maclay G J 1998 *J. Appl. Phys.* **84** 2501–6
[94] Chan H B, Aksyuk V A, Kleiman R N, Bishop D J and Capasso F 2001 *Science* **291** 1941–4
[95] Chan H B, Aksyuk V A, Kleiman R N, Bishop D J and Capasso F 2001 *Phys. Rev. Lett.* **87** 211801
[96] Decca R S *et al* 2003 *Phys. Rev. Lett.* **91** 050402
[97] Bressi G *et al* 2002 *Phys. Rev. Lett.* **88** 041804
[98] Iannuzzi D, Lisanti M and Capasso F 2004 *Proc. Natl Acad. Sci.* **101** 4019–23
[99] Boersma S L 1996 *Am. J. Phys.* **64** 539–41
[100] Hawking S W 1975 *Commun. Math. Phys.* **43** 199–220
[101] Hawking S W 1977 *Sci. Am.* **236** 34–40
[102] Unruh W G 1976 *Phys. Rev.* D **14** 870–92
[103] Davies P C W 1975 *J. Phys.* A **8** 609
[104] Boyer T H 1985 *Sci. Am. Aug.* **1985** 75–8
[105] Rudolf Peierls 1979 *Surprises in Theoretical Physics* (Princeton, NJ: Princeton University Press)
[106] Schwinger J 1994 *Proc. Natl Acad. Sci. USA* **91** 6473–5
[107] Brevik V, Marachevsky V N and Milton A K 1999 *Phys. Rev. Lett.* **82** 3948
[108] Bourne N K and Field J E 1999 *Phil. Trans.* A **357** 295
[109] Chakravarty A and Walton A J 2000 *J. Luminescence* **92** 27
[110] Xu N, Wang L and Hu X 1999 *Phys. Rev. Lett.* **83** 2441
[111] Sir Edmund Whittaker 1960 *A History of the Aether and Electricity* vol 1 (New York: Harper Torchbook)
[112] Loomis J J and Maris H J 1994 *Phys. Rev.* B **50** 18517–24
[113] Ibach H and Mills D L 1982 *Electron Energy Loss Spectroscopy and Surface Vibrations* (New York: Academic) Chapter 3
[114] DiMatteo R S *et al* 2001 *Appl. Phys. Lett.* **79** 1894–5
[115] Varpula T and Poutanen T 1984 *J. Appl. Phys.* **55** 4015–21
[116] Lamoreaux S K 1999 *Phys. Rev.* A **60** 1717–20
[117] Lamoreaux S K 1997 *Phys. Rev.* A **56** 4970–5
[118] Henkel C and Wilkens M 1999 *Europhys. Lett.* **47** 414–20
[119] Fischbach E and Talmadge C 1996 *Proc. XXXI Recontres de Moriond (Les Arcs, 20–27 January 1996)* ed R Ansari *et al* (Gif-Sur-Yvette: Editions Frontieres) p 443
[120] Long J C, Chan H W and Price J C 1998 *Nucl. Phys.* B **539** 23–34
[121] Bordag M, Gillies G T and Mostepanenko V M 1997 *Phys. Rev.* D **56** R6–R10
Bordag M, Gillies G T and Mostepanenko V M 1998 *Phys. Rev.* D **57** 2024
[122] Schiff L 1941 *Phys. Rev.* **59** 839
[123] Dzyaloshinskii I E, Lifshitz E M and Pitaevskii L P 1961 *Adv. Phys.* **10** 165
[124] Sabinsky E S and Anderson C H 1973 *Phys. Rev.* A **7** 790
[125] Cheng E, Cole M W, Saam W F and Treiner J 1991 *Phys. Rev. Lett.* **67** 1007–10
[126] Nacher P J and DupontRoc J 1991 *Phys. Rev. Lett.* **67** 2966–9
[127] Elbaum M 1991 *Phys. Rev. Lett.* **67** 2982–5
[128] Elbaum M, Lipson S G and Dash J G 1993 *J. Cryst. Growth* **129** 491–505
[129] Elbaum M and Schick M 1991 *Phys. Rev. Lett.* **66** 1713–16
[130] Bostrum M and Sernelius Bo E 1999 *Appl. Surf. Sci.* **142** 375–80